universität wien

DIPLOMARBEIT

Titel der Diplomarbeit

Preparation and quality control of [^{18}F]Fallypride for PET neuroimaging of dopamine D_2-like receptors

angestrebter akademischer Grad

Magister der Pharmazie (Mag.pharm.)

Verfasserin / Verfasser:	Michael Zeier
Matrikel-Nummer:	0256327
Studienrichtung (lt. Studien-blatt):	Diplomstudium Pharmazie A449
Betreuerin / Betreuer:	O.Univ.-Prof. Mag.pharm. Dr. Helmut Viernstein

Wien, am 23.10.2011

Acknowledgments

I would like to thank my supervisor O.Univ.-Prof.Dr. Helmut Viernstein for offering the chance of conducting this diploma thesis at the General Hospital of Vienna.

My gratitude goes to O.Univ.-Prof. Dr. Robert Dudczak and Univ.-Prof. DDr. Kurt Kletter for making available the lab workspace at the university clinic of Nuclear Medicine at the general hospital of Vienna.

I would like to thank Ass.-Prof.Dr. Markus Mitterhauser and Ass.-Prof.Dr. Wolfgang Wadsak for sparking my interest in radiochemistry. Their comprehensive support during all stages of this work shall be especially emphasized.

Special thanks go to Mag.[a] Johanna Ungersböck for being such a warm-hearted and capable advisor. Thanks to Dr. Leonhard-Key Mien for being the incredibly positive and helpful person he is.

My gratitude goes to Mag.[a] Daniela Häusler, Mag. Lukas Nics, Mag.[a] Cécile Philippe, and Markus Zeilinger, BSc for creating an enjoyable working environment and for always having an open ear for my questions.

Additional thanks go to Dr. Harald Eidherr and Friedrich Gierschele for supporting me during lab work.

Last, but not least I would like to thank my family for always supporting me in many ways. Without you, this thesis would not have been possible.

Also, I would like to thank my fellow students Burnie, Lisi, Martin, Paolo, Sigrid and Shu. I'm glad to have you as friends and I always enjoyed spending countless hours studying with you in one of Vienna's libraries.

Table of contents

Abstract

Objectives: The imaging of dopamine D_2 receptors is essential for the diagnostic assessment of diseases in which the dopaminergic system is affected. (e.g. Parkinson's disease, Chorea Huntington and schizophrenia)

First generation dopamine D_2 radiotracers like [^{123}I]IBZM and [^{11}C]Raclopride showed only moderate affinity towards the dopamine D_2 receptor, making the imaging of these receptors in extrastriatal brain areas impossible. High-affinity dopamine D_2 receptor tracers like [^{18}F]Fallypride have been designed to make extrastriatal dopamine D_2 receptors accessible to PET neuroimaging.

This diploma thesis focuses on the optimization of two radiosynthesic approaches for the synthesis of [^{18}F]Fallypride. The first approach was „conventional" vial-based radiosynthesis, while in the second approach a microfluidic chemistry device (the Advion® NanoTek LF) was used. Furthermore, radio-TLC (thin layer chromatography) and radio-HPLC (high pressure liquid chromatography) assays were developed to detect, identify and quantify [^{18}F]fluoride, [^{18}F]Fallypride and potential by-products of the synthesis.

Methods: [^{18}F]fluoride was obtained in its aqueous solution by irradiation of [^{18}O]water in a GE PETtrace medical cyclotron utilising the ^{18}O (p,n) ^{18}F nuclear reaction. To increase its nucleophilicity, [^{18}F]fluoride was separated from [^{18}O]water by adsorption onto an anion exchange cartridge. [^{18}F]fluoride was transferred into the organic phase through elution with a solution of potassium carbonate and the phase transfer catalyst Kryptofix 2.2.2. in water / acetonitrile (70/30 v/v%). Trace water was then removed by azeotropic drying and re-solution of [^{18}F]fluoride in acetonitrile under inert gas atmosphere.

[^{18}F]Fallypride was synthesized from its tosylate precursor by nucleophilic substitution of the tosylate group by means of (1) addition of a solution of [^{18}F]fluoride to a solution of the tosylate precursor and subsequent heating in a glass vial. (2) using a novel microfluidic synthesis device. Reactions were performed within this microfluidic system

by simultaneously pushing [^{18}F]fluoride and tosylate precursor through the fused-silica micro-reactor.

The radiosynthesis of [^{18}F]Fallypride was evaluated in respect to optimal reaction conditions (e.g. concentration, reaction duration and reaction temperature) for both approaches.

Results: Optimum reaction conditions for the vessel-based synthesis of [^{18}F]Fallypride were a precursor concentration of 2.5mg/mL and a reaction duration of 30 minutes at a temperature of 70°C, yielding 35.6±4.2% of the product [^{18}F]Fallypride. For microfluidic syntheses, ideal reaction conditions were a precursor concentration of 2.5mg/mL at a reaction temperature of 180°C and a flow rate of 30µL/min per pump (60µL/min overall flow rate), yielding 91.6±1.0% of the product [^{18}F]Fallypride.

Conclusion: Optimized reaction conditions and quality control procedures for the synthesis of [^{18}F]Fallypride have been established for the classic vessel-based approach as well as the microfluidic synthesis approach. Very high yields, low precursor usage and short reaction times of microfluidic reactions show the importance of this emerging new technique in radiosynthesis, especially for hardly available and expensive precursors.

Zusammenfassung

Ziele: Die Bildgebung von Dopamin D_2-Rezeptoren ist essentiell für die nuklearmedizinische Diagnostik von Erkrankungen mit Beteiligung des dopaminergen Systems wie der Parkinson'schen Krankheit, Chorea Huntington und der Schizophrenie.

Da Dopamin D_2 Rezeptortracer der ersten Generation wie [^{123}I]IBZM oder [^{11}C]Raclopride nur moderate Affinitäten zum D_2-Rezeptor zeigen, war mit diesen Substanzen eine Darstellung von D_2-Rezeptoren in extrastriatalen Hirnarealen nicht möglich. Hochaffine D_2-Liganden wie [^{18}F]Fallypride ermöglichen hingegen die Darstellung von D_2-Rezeptoren in diesen Gehirnarealen.

Diese Diplomarbeit beschäftigt sich mit der Optimierung zweier Ansätze zur Synthese des PET-Radiotracers [^{18}F]Fallypride. Zuerst wurde [^{18}F]Fallypride mittels nasschemischer Methoden synthetisiert. Danach erfolgte die Synthese von [^{18}F]Fallypride mittels eines neuartigen Mikrofluidsystems, dem Advion® NanoTek LF. Weiters wurden ein radio-dünnschichtchromatographisches Verfahren und eine radio-HPLC-Methode für die Qualitätskontrolle und zur Erkennung potentieller Verunreinigungen entwickelt.

Methoden: [^{18}F]Fluorid wurde in einem GE PETtrace-Zyklotron durch Bestrahlung von [^{18}O]Wasser unter Anwendung der ^{18}O (p,n) ^{18}F-Kernreaktion in wässriger Lösung gewonnen. Um die Nukleophilie des [^{18}F]Fluorids zu erhöhen, wurde es durch Adsorption an eine Anionenaustauscherkartusche von [^{18}O]Wasser abgetrennt und mittels einer Lösung aus Kaliumcarbonat und dem Phasentransferkatalysator Kryptofix K.2.2.2 in Acetonitril/Wasser (70:30 v/v%) in die organische Phase übergeführt. Durch azeotrope Trocknung unter Inertgas wurden letzte Wasserspuren entfernt.

[^{18}F]Fallypride wurde sodann durch nukleophile Substitution der Tosylatgruppe aus dem Precursor tosyl-Fallypride synthetisiert, indem eine Lösung von getrocknetem [^{18}F]Fluorid zu einer Lösung des Precursors hinzugegeben und in einem Aluminiumheizblock erhitzt wurde. Die Synthese von [^{18}F]Fallypride im Mikroreaktor erfolgte durch gleichzeitiges Einleiten von [^{18}F]Fluorid und der Vorläufersubstanz tosyl-Fallypride in den erhitzten Mikroreaktor.

Die Radiosynthese von [^{18}F]Fallypride wurde für beide Ansätze hinsichtlich optimaler Precursorkonzentration, Reaktionsdauer und Reaktionstemperatur evaluiert.

Ergebnisse: Optimale Synthesebedingungen für den nasschemischen Ansatz wurden unter Verwendung einer Precursorkonzentration von 2.5mg/mL, einer Reaktionsdauer von 30min bei einer Reaktionstemperatur von 70°C erzielt. Die radiochemische Ausbeute betrug hierbei 35,6±4,2% des Produkts [^{18}F]Fallypride. Für die mikrofluidischen Synthesen erwiesen sich eine Precursorkonzentration von 2.5mg/mL bei einer Reaktionstemperatur von 180°C und einer Durchflussrate von 30µL/min pro Pumpe (Gesamtdurchflussrate: 60µL/min) als ideal, wobei sich sehr hohe Ausbeuten von 91.6±1.0% ergaben.

Schlussfolgerung: Sowohl für die klassische “Kessel”-Reaktion als auch für den mikrofluiden Ansatz wurden ideale Reaktionsbedingungen für die Synthese von [^{18}F]Fallypride etabliert. Ausgezeichnete Ausbeuten, geringer Precursorverbrauch und kurze Reaktionszeiten der mikrofluiden Reaktionen verdeutlichen die Wichtigkeit dieser Technik für Radiosynthesen, speziell für schwer erhältliche und teure Vorläufersubstanzen.

1 Introduction

1.1 Basic considerations on radioactivity

The analysis of the naturally occurring radioelements Thorium and Radium beared the insight that some “elements” are not separable by chemical means. [1] This finding led to the concept of isotopes (Greek: “in the same place”).

Atoms differing by their atomic number or mass number are called nuclides. For identification, element symbol and mass number are used. [2]

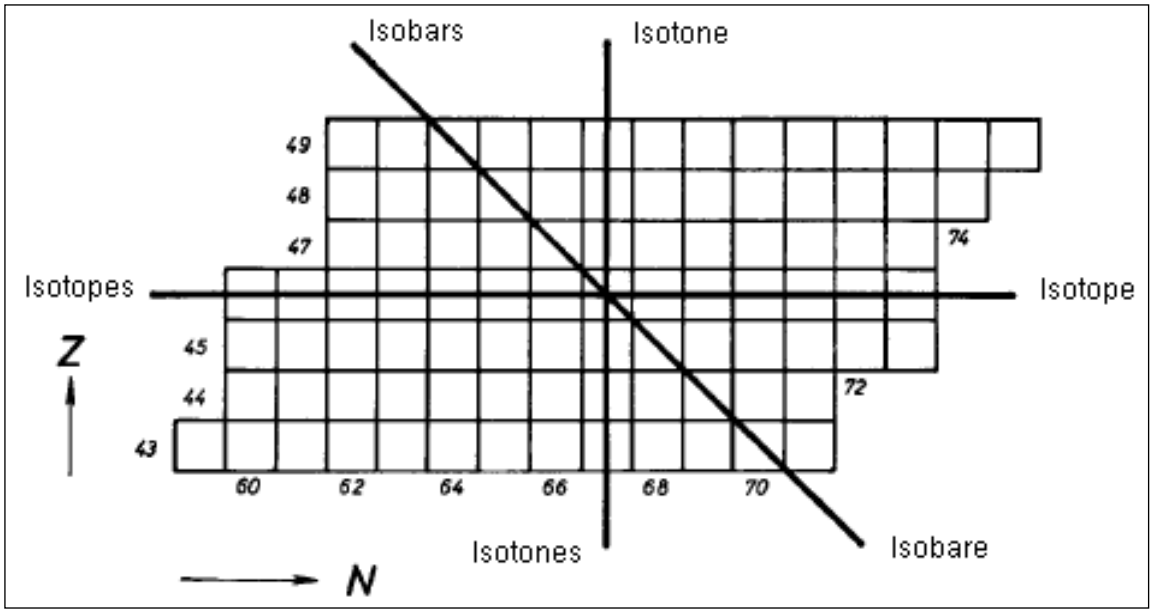

Fig. 1.1: The chart of the nuclides, graphical depiction of important terms (from [3])

Isotopes of an element exhibit the same number of protons in their nuclei, but the number of neutrons is different. For this reason the chemical properties of isotopes are identical, and they occupy the same place in the periodic table of elements. The periodic table does not have room for information about all the isotopes. For this reason the chart of nuclides has been designed. In such a chart, the nuclides are placed in a diagram: the ordinate represents the number of protons (Z) whereas the abscissa represents the number of neutrons (N).

In the chart of the nuclides, stable nuclides are arranged around a line starting at the point of origin. This line, which is called the line of β stability, has the slope 1,

which means N equals Z for the nuclides on the line. For heavier nuclides, the line is bent towards the abscissa. This is because the nuclear attractive force neutrons exert onto other nucleons (the so-called “strong force”) is very short ranged (effective only at distances smaller than 2.4fm).[4]

Neutrons can only interact with their nearest neighbour nucleons. On the contrary, the repulsive Coulomb force the positively charged protons exert onto each other is much more long-ranged. (decreasing proportionally to $1/r^2$) For this reason, the number of neutrons has to grow faster than the number of protons for a nucleus to be stable.

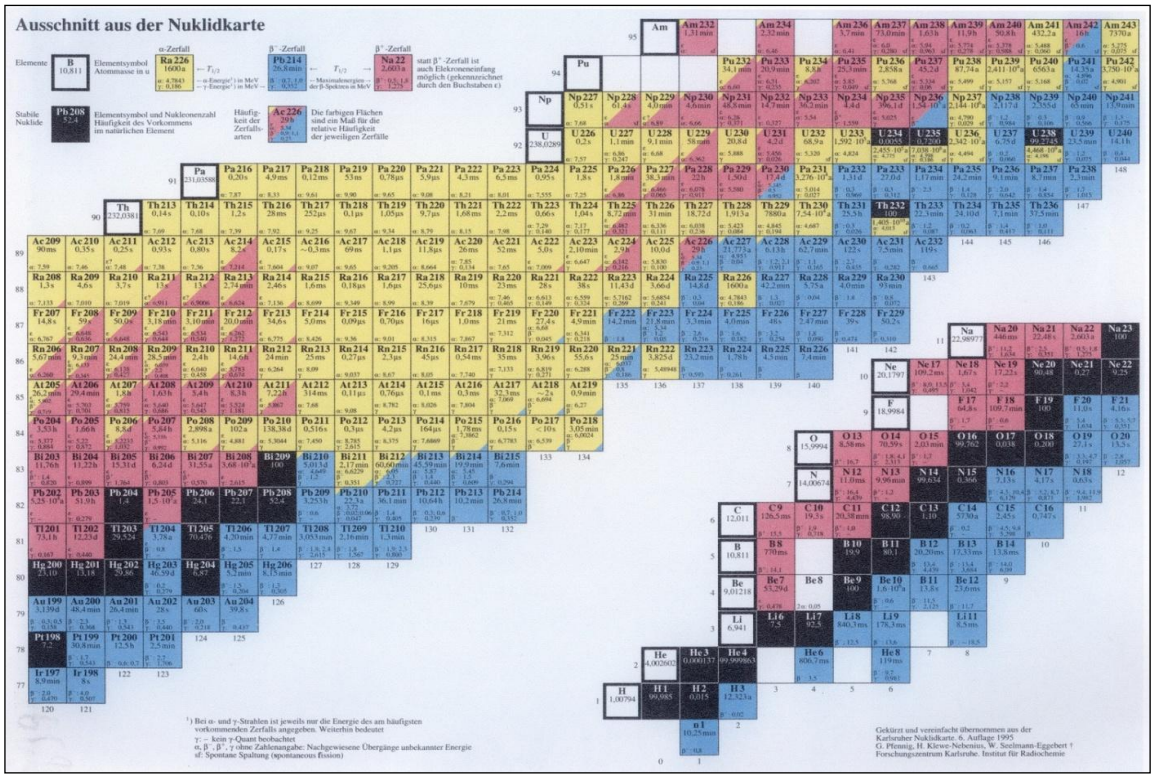

Fig. 1.2: A section of the Karlsruhe nuclide chart, depicting the line of β-stability (black boxes) and the different decay modes (red, blue, yellow and white boxes) from [5]

Nuclides not on or near the line of β stability are unstable and decay in various modes and are thus called radionuclides. These are color-coded in the chart of nuclides (Fig. 1.2).

1.2 Radioactive decay

Radioactive decay is the spontaneous transmutation of an unstable parent nucleus into a stable or unstable daughter nucleus, whereas the released energy is emitted in the form of α or β particles and/or γ rays. Depending on the properties of the nuclide, various decay modes can occur.

1.2.1 α decay

The process of α decay is found preferably in proton rich, heavier elements due to the fact that electrostatic repulsive forces increase more rapidly in heavy nuclides than cohesive nuclear forces. [3] These nuclides are coded yellow in the Karlsruhe nuclide chart (Fig. 1.2), their mode of decay is described by the following equation:

$$ {}^{A}_{Z}P \rightarrow {}^{A-4}_{Z-2}D + {}^{4}_{2}He^{2+} $$

Due to their size, α particles are not easily deflected. On their way through tissue, α particles cause ionizations through electrostatic attraction of electrons. The α particle's energy is deposited along the traversed tissue until two electrons are captured, leading to the formation of a neutral helium atom. The amount of energy deposited per unit distance, called linear energy transfer (LET), is however bigger than for β or γ radiation. [6]

For this reason, the cytotoxicity of α radiation is greater than that of β or γ radiation. Additionally, energy deposition of α radiation is locally delimited due to the average range of less than 100µm in tissue. [6]

These advantageous characteristics make α emitters (e.g. Astatine-211) subject to intense research as therapeutic nuclides for various applications in radiotherapy.

1.2.2 β^--decay

β^--decay is the emission of an electron (β^-) and an anti-neutrino (ν) from an unstable parent nucleus P. Formally, this process is described as follows:

$$ {}^{A}_{Z}P \rightarrow {}^{A}_{Z+1}D + \beta^{-} + \overline{\nu} $$

This decay form occurs with nuclei exhibiting an excess of neutrons. In the nucleus, a neutron is converted into a proton, an electron β^- and a neutrino. To emphasize the origin of the electron is the nucleus, it is denoted β^- while electrons from atomic shells are denoted e^-.

Nuclei decaying through β^- decay are coded blue in the Karlsruhe nuclide chart. (Fig. 1.2) β^--emitters are used as therapy nuclides in targeted radiotherapy. Since β^- radiation produces very few ionizations along the beam track and almost all particle energy is deposited within the last few nanometers of the particle range, it allows the locally delimited delivery of high radiation doses to malignant tissue.[6]

An example for a β^- emitter is Iodine-131, which is used for the radiotherapy of the thyroid. Other beta-minus emitting nuclides are Lutetium-177, Rhenium-188 and Yttrium-90, all are used in the targeted radiotherapy of malignant diseases.

1.2.3 β^+ decay

Beta-plus or positron decay occurs with nuclides with an excess of protons. These nuclides are color coded red in the Karlsruhe nuclide chart. This process is defined by the following equation:

$$ {}^{A}_{Z}P \rightarrow {}^{A}_{Z-1}D + \beta^{+} + \nu $$

A proton in the nucleus is converted into a neutron, while a positron β^+ (a positively-charged electron) and a neutrino are ejected from the nucleus. The positron is strongly attracted by the negative charges of adjacent electrons. Positron and electron annihilate into two γ photons with an energy of 511keV each after their collision. These γ-photons are then emitted in exactly opposed directions although minor deviatons have been reported. [7]

Positron emitters as ^{11}C, ^{13}N, ^{18}F or ^{68}Ga are widely used in nuclear medicine, as they are the basis for PET imaging, which is discussed in detail in chapter 1.5.

1.2.4 Electron capture (EC) or ε decay

Just as β^+ decay, EC decay occurs in proton-rich nuclides. A nucleus captures an electron from its shell, most commonly the K shell. The core proton and the captured electron are converted into a neutron and an electron-neutrino.

The position of the K shell electron is immediately filled by an electron from a higher shell, while the energy difference between the shells is emitted as monoenergetic X rays. [8]

The EC decay process is described by the following equation:

$$ {}^{A}_{Z}P + {}^{0}_{-1}e^{-} \rightarrow {}^{A}_{Z-1}D + {}^{0}_{0}\nu_e $$

1.2.5 γ transitions

When an unstable nucleus decays through α ,β or EC decay, the daughter nucleus will often not result directly in its energetic ground state, but in a state of excess energy. Therefore, the nucleus has to emit this excess energy in the form of γ rays.

Often this emission consists not only of a single γ quantum but a cascade of γ transitions with different transition energies until the ground state is reached. Since these states possess discrete energy levels, the emitted γ photons are also of discrete energies.

When γ rays are detected with a scintillation counter and the count rate is plotted versus energy, a γ energy spectrum (e.g. Fig. 1.3) results. Since this spectrum is unique for every nuclide, γ spectroscopy can be used for radionuclide identification.

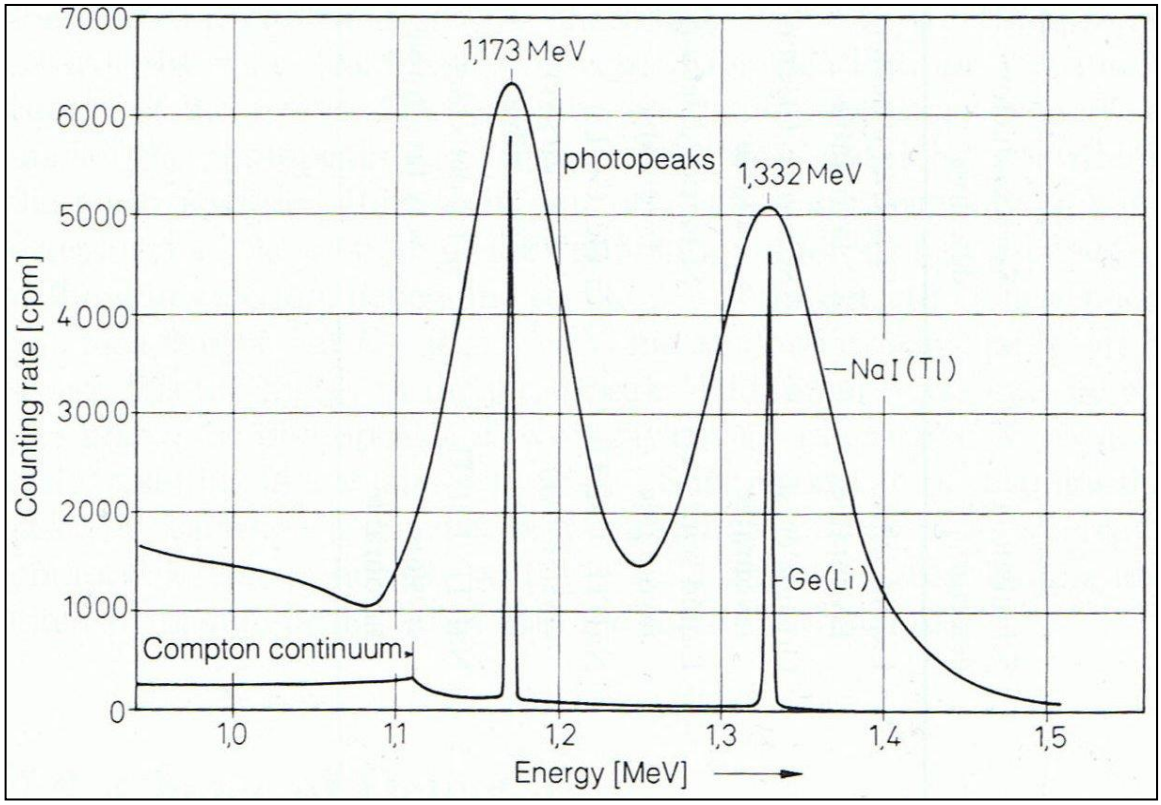

Fig. 1.3: γ energy spectrum of ^{60}Co (from [9])

The most prominent applications of γ-emitters in nuclear medicine are scintigraphy and SPECT, both are discussed in chapter 1.4.2.

1.3 Production of radionuclides for nuclear medicine

Radionuclides used in nuclear medicine are produced artificially either by means of nuclear reactors, nuclide generator systems or particle accelerators.

1.3.1 Radionuclide production via nuclear reactors

Neutron-rich radionuclides can be obtained by irradiation of the target material with a neutron beam. This beam is generated through the fission of heavy, neutron-rich nuclides such as ^{235}U in a nuclear reactor. After a ^{235}U nucleus captures a neutron, it splits into two medium-weight nuclei, while an average 2.4

neutrons are released. [10] These neutrons can subsequently be captured by other ^{235}U nuclei and thus sustain the nuclear fission chain reaction.

Since the reaction cross section (the probability for a nuclear reaction to occur) is highest for thermal neutrons with kinetic energy of up to 0.025eV [11], fast neutrons (neutrons possessing kinetic energies greater than 100keV) released during the nuclear fission reaction have to be decelerated to “thermal” velocities with kinetic energy of less than 0.4eV) to increase the probability for nuclear reactions. [12]

For this task a moderator like water, deuterated water or graphite is used. Fast neutrons are slowed down to a thermal energy level through collisions with moderator atoms. After neutron energy has been reduced to a thermal level, the target material can be placed in the neutron beam to obtain the desired radionuclide.

Prominent examples for radionuclides manufactured in nuclear reactors are ^{3}H, ^{14}C, ^{131}I, ^{99}Mo and ^{68}Ge.

1.3.2 Radionuclide production via nuclide generators

Since the importance of ^{99m}Tc for medical imaging was recognized, the demand for high purity, easy to handle production of ^{99m}Tc has been constantly rising. Out of this need, Tucker, Richards and Green developed the ^{99}Mo / ^{99m}Tc radionuclide generator system in 1958. [13]

In this system, the long-lived mother nuclide ^{99}Mo is adsorbed onto an ion exchange resin, steadily decaying into its daughter nuclide ^{99m}Tc. When activity levels of mother and daughter nuclide reach equilibrium, the generator column is eluted with 0.9% saline solution to separate both nuclides from one another.

During the elution process, the pertechnetate anion $[^{99m}Tc]TcO_4^-$ is displaced by the Cl^- anion by means of anion exchange. The activity of daughter nuclide in the column is thereby reduced to almost zero. New daughter grows out of the mother

nuclide, reaching equilibrium with the mother once again after a certain period of time, at which the generator can be eluted again. (shown in Fig. 1.4)

The available daughter activity decreases linearly with the decay of the mother nuclide. Depletion of the mother nuclide marks the end of the generator's life-span.

Apart from ^{99m}Tc used in γ scintigraphy, also some PET nuclides can be obtained from generator systems. Gallium-68, which for example is used for the labelling of peptides for PET imaging of neuroendocrine tumors can be obtained from its mother nuclide ^{68}Ge in the ^{68}Ge / ^{68}Ga generator system. Another example for a generator PET nuclide is ^{82}Rb (used for myocardial perfusion studies) obtained from ^{82}Kr using the ^{82}Kr / ^{82}Rb generator system.

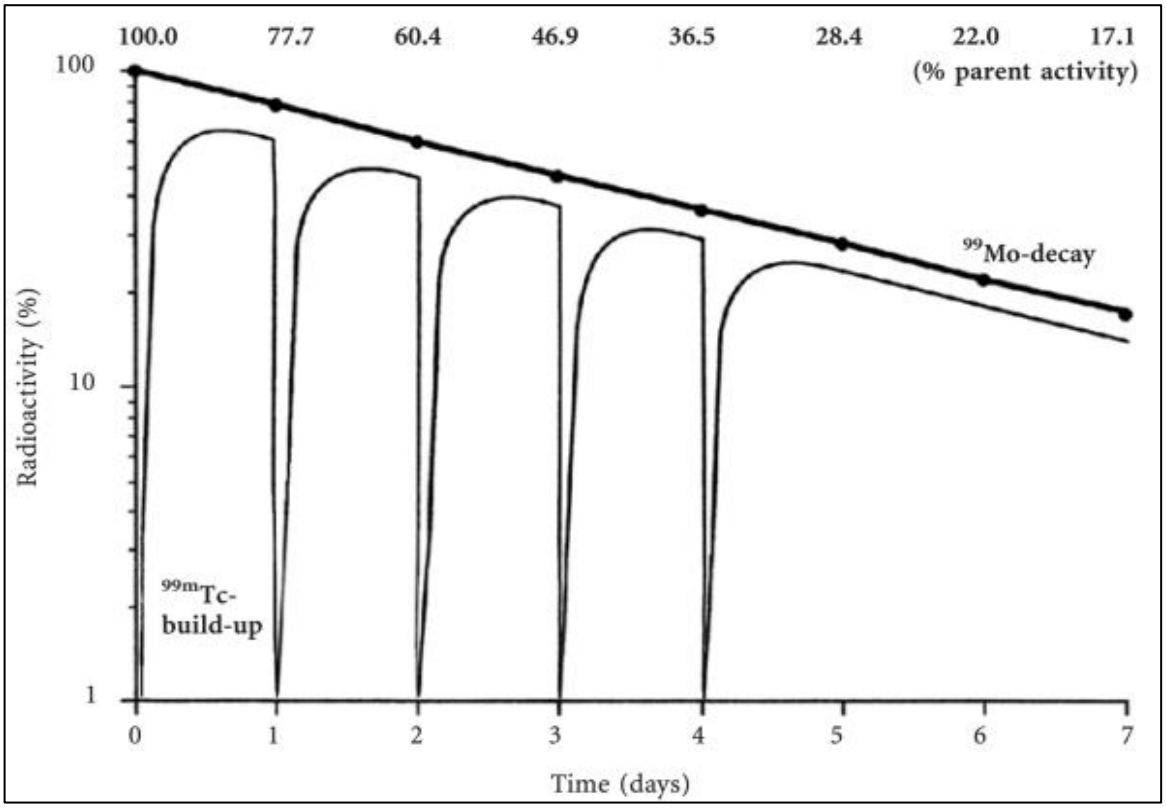

Fig. 1.4: Activity relationships in a ^{99}Mo / ^{99m}Tc nuclide generator system (from [14])

For reasons of easy handling and almost instant radionuclide availability, generator systems have found a broad application in nuclear medicine, not least because of the independence from a costly cyclotron for radionuclide production.

1.3.3 Radionuclide production via cyclotron

Common proton-rich PET nuclides like ^{18}F, ^{11}C, ^{13}N or ^{15}O are produced by bombarding suitable target nuclei with a proton or deuteron beam in a cyclotron.

A cyclotron is a circular accelerator comprised of an ion source, a solenoid with two D-shaped chambers (“Dees”) between its poles and a chamber containing the target material. These chambers are evacuated to prevent loss of kinetic energy and unwanted nuclear reactions with nuclei present in the air.

A uniform magnetic field is applied to force the particles on a semicircular orbit within the Dee. Since the Dees are shielded, only the magnetic force can affect the particles inside. When the gap between the Dees is reached, the electrical field gradient is reversed to accelerate the particles.

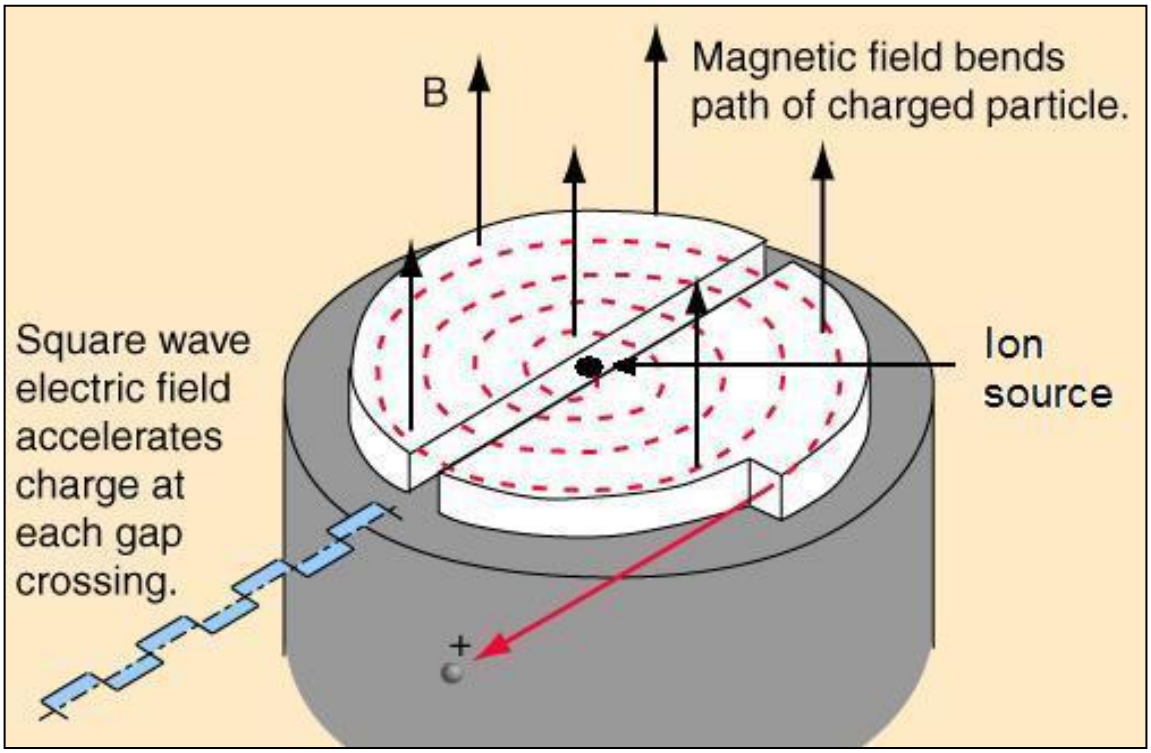

Fig. 1.5: Schematic illustration of a cyclotron particle accelerator (modified after [15])

Since the time a particle needs to traverse its orbit is independent of the orbit radius [16] the frequency at which the electrical field phase in the gap changes (the cyclotron frequency) can be kept constant throughout the whole acceleration process. When the particle beam has gained sufficient energy and orbit radius, it reaches a carbon foil which “strips off” electrons from the accelerated H^- ions, turning them into H^+ ions. Since the orientation of the electric field has not changed, the H^+ ions are being deflected towards the outlet opening and directed into the target chamber.

In the target chamber, the high-energy protons collide with the target material to form the desired radionuclide in a transmutation reaction. The most common transmutation reaction used in a medical cyclotron is the reaction of oxygen-18 with a proton to form fluorine-18. [17] This transmutation reaction is shown in Fig. 1.6.

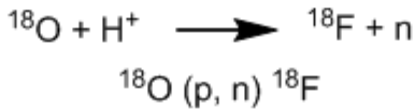

Fig. 1.6: Production of [^{18}F]fluoride from [^{18}O]H_2O in a cyclotron

1.4 Conventional Nuclear Imaging

Nuclear medicine uses radioactive compounds for diagnostic or therapeutic applications. These methods often allow the diagnosis of a disease before morphologic changes in body tissue become visible.

The major difference between the techniques of nuclear medicine and other imaging techniques is that the former deliver *functional* information, while the latter deliver *structural* information about the examined tissue or organ. In conjunction with other imaging techniques, a comprehensive picture of the organ status, structural and functional, can be gained.

Conventional imaging techniques include ultrasound, x-ray, computed tomography (CT) and magnetic resonance tomography (MRT). Nuclear imaging techniques include scintigraphy, single photon computed tomography (SPECT)

and positron emission tomography (PET). All nuclear methods make use of radioactively labelled compounds that are administered (mostly intravenously) to the patient, so-called *radiopharmaceuticals*.

1.4.1 Radiopharmaceuticals

Radiopharmaceuticals are composed of a ligand, a chemical structure determining its affinity to a target structure in the human body, and one or more unstable atoms linked to the ligand. They are used either for diagnostic imaging or for endoradiotherapy in nuclear medicine.

A radiopharmaceutical is applied to the patient through injection, distributes throughout the body and accumulates in its target tissue or organ.

The distribution of the emitted radioactivity in the body can be detected by a scanner and transformed into an image of the examined region using various techniques. The radiation released during the decay of the radioactive atom can be used for diagnostic or therapeutic purposes, depending on the physical properties of the used radionuclide. (e.g. half-life and energetic characteristics of the emitted radiation)

Radionuclides used for diagnostic purposes are γ emitters in scintigraphy and SPECT or, due to their annihilation into γ photons, β^+ emitters in PET. The diagnostic value of γ emitters is their minor interaction and long range in tissue, which makes this type of radiation detectable outside the body.

Radiopharmaceuticals used for endoradiotherapy are meant to specifically target and irradiate malignant tissue in order to destroy it. For this purpose, nuclides emitting radiation with a high grade of tissue interaction, like α, β^- or Auger electron emitters are coupled to a ligand providing affinity to the tumor tissue. Depending on the size and localization of the tumor, nuclides with different maximum energies and ranges can be used. A selection of therapeutically used nuclides is presented in Table 1.1.

Nuclide	Half-life	Decay Mode	Max. Energy	Max. Range
^{68}Ga	3.3d	EC	<0.1MeV	<10nm
^{211}At	7.2h	α, EC	6.8MeV	65µm
^{177}Lu	6.7d	β^-, γ	0.5MeV	1.5mm
^{90}Y	2,7d	100% β^-	2.3MeV	12mm

Table 1.1: Therapeutically used radionuclides (data from [18])

1.4.2 Scintigraphy and SPECT

Radiopharmaceuticals used in scintigraphy contain γ emitting nuclides such as ^{99m}Tc or ^{131}I. The radiation emitted by the radiotracer is detected by a γ camera. This device contains an array of scintillation crystals which emit flashes of light when hit by γ rays. The emitted flashes are detected by photomultiplier tubes and the number of counts is summed up by a connected computer system.

Based on the collected data a two-dimensional image of the spatial count density is computed, in which different shades of color represent different amounts of detected counts. This diagram represents the distribution of the radiotracer concentration in the examined area.

SPECT is very similiar to scintigraphy. The major difference is that the γ camera rotates around the patient. It collects sectional images which are later transformed into a three-dimensional model of the examined area. In Fig. 1.7, the result of a thyroid scintigraphy (a scintigram) using [^{99m}Tc]TcO_4^- is shown.

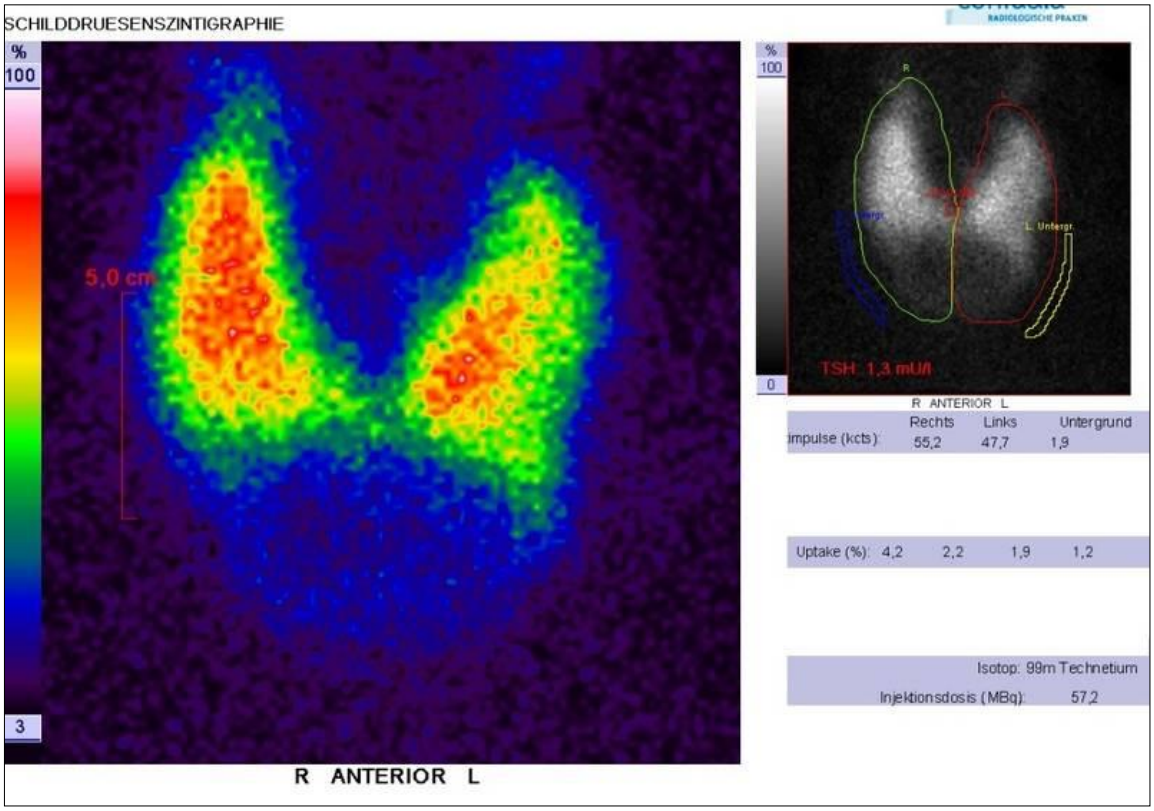

Fig. 1.7: Thyroid scintigraphy showing struma (from [19])

1.5 Positron emission tomography

In contrast to scintigraphy and SPECT, PET relies on the detection of γ photons generated through positron annihilation. The result of this measurement over time is a quantitative representation of the distribution of radioactivity in the observed tissue or organ.

Since only coinciding γ photons are detected, annihilation events can be assigned to a unique spatial position in the observed area, making PET image resolution superior to that of other nuclear imaging techniques.

1.5.1 Functionality of a PET scanner

The basis for PET imaging is the detection of γ quanta formed during positron annihilation. A positron emitted by the radiopharmaceutical loses its kinetic energy through ionizations and excitation of atoms along its pathway until it reaches thermal velocities and combines with an orbital electron. [20] The

masses of the two particles are converted into γ photons, each of 511keV energy. These photons are emitted at an angle of almost exactly 180 degrees, although deviations have been reported. [7]

Taking into account the four most important PET nuclides (i.e. Carbon-11, Nitrogen-13, Gallium-68 and Fluorine-18), a positron covers a distance of maximum 8mm before annihilation. Therefore, the spatial resolution of PET is limited to the maximum range of the respective nuclide.

1.5.2 Detection of positron annihilation in PET

The mode of positron annihilation detection is a unique advantage of PET in comparison to other nuclear imaging techniques. Since two photons are emitted simultaneously at an angle of 180 degrees, they should (if originating from the same annihilation event) arrive almost at the same time at the two opposed detectors.

Only if both opposed detectors are activated in a small frame of time, a coincidence is registered. It is however possible that independent γ photons are falsely recognized as coincidences. In Table 1.2, three types of coincidences are distinguished. Two of them ("scatters" and "randoms") may lead to the false assignment of a line of response (LOR), decreasing image quality. These three types of coincidences are depicted graphically in Fig 1.8.

Type of coincidence	Description
true	the detected photons originate from a pair annihilation event, the assigned LOR (line of response) is correct.
scatter	a photon has undergone scattering, but both photons arrive at opposed detectors at the same time, which results in an incorrect LOR.
random	two photons from different events are detected in opposed detectors simultaneously. The assigned LOR is incorrect.

Table 1.2: Consequences of positron scattering for PET image reconstruction

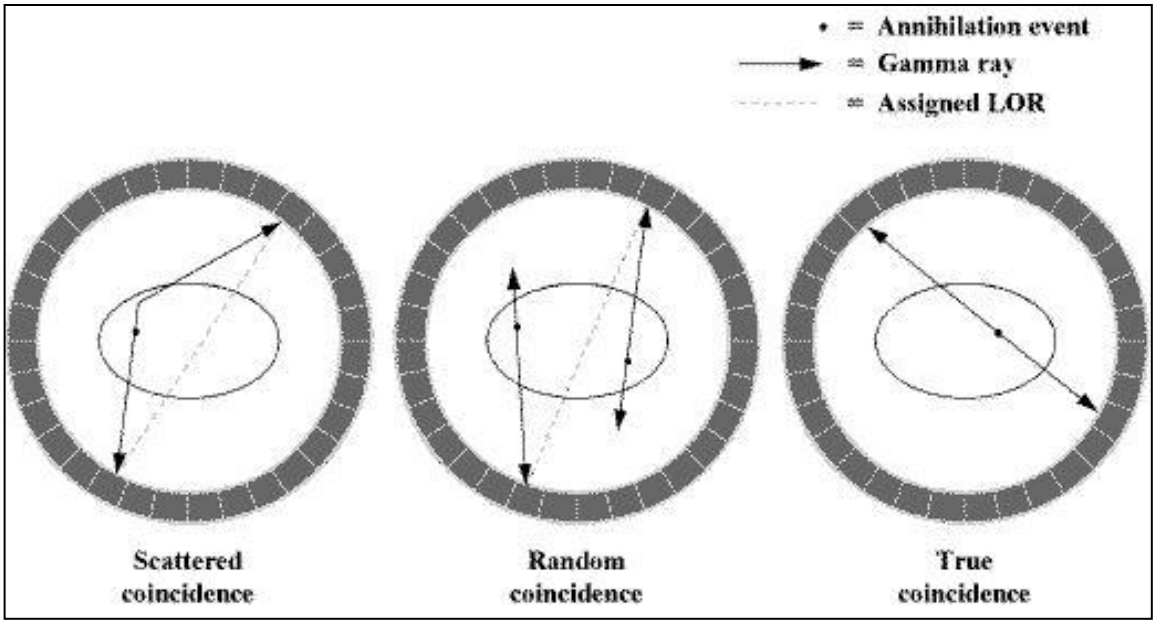

Fig. 1.8: Types of coincidences in PET (from [21])

Another factor for decreased image quality is tissue attenuation. To register an annihilation event correctly, both photons must leave the body unattenuated. Since photons originating from deeper body compartments have to traverse body tissue, these photons are far more likely attenuated on their way through the body. In opposite, events from the outer layers of the body are far less likely attenuated, which results in above-average count-rates for events originating in outer body layers.

This problem can be solved through attenuation correction. An additional scan is performed with a radiation source along all possible LORs [21] to obtain attenuation data of the examined region. The attenuation data can be applied to the uncorrected image to receive correct count densities.

1.5.3 Radionuclides used in PET radiopharmaceuticals

All radionuclides used in PET radiopharmaceuticals are neutron-deficient positron emitters. Properties of the most frequently used nuclides are shown in Table 1.3.

Nuclide	Half-life (min)	Decay mode	Particle energy
C-11	20.38	β^+	0.960 MeV
N-13	9.96	β^+	1.19 MeV
Ga-68	67.62	β^+ / γ	1.83 /1.077 MeV
F-18	109.8	β^+	0.635 MeV

Table 1.3: The four most important PET nuclides and their characteristics (data from [22],[23])

Carbon-11 can be used to *isotopically* label a compound. Since carbon occurs in every organic molecule, carbon-12 can be exchanged for carbon-11 without affecting the physicochemical parameters and biological behaviour of the molecule.

Due to their very short half lifes, the use of nitrogen-13 and oxygen-15 is restricted to very basic synthetic procedures. Since blood flow is a “fast process” in contrast to metabolism or receptor equilibrium processes, the short half-lifes of oxygen-15 and nitrogen-13 are sufficient to perform blood perfusion measurements of the brain and the myocardium.

Fluorine-18 is a very common nuclide in radiochemistry. Its half-life of 109.8 minutes allows its use in multi-step syntheses, the observation of slowly equilibrating processes, and its shipping to satellite medical facilities.[24]

Its maximum positron energy of 0.635 MeV results in a comparatively low radiation burden for the patient and a maximum range of 2.4mm in the human body. [22] For this reason, the spatial resolution of PET scans using a [^{18}F]fluorine-labelled radiotracer is superior to scans performed with other radionuclides.

Another advantage of a [^{18}F]fluorine label is that its atom radius is very similar to that of a hydrogen atom. [25] Therefore, a hydrogen atom can be substituted with [^{18}F]fluorine without much steric alteration of the molecule.

The only downside to fluorine-18 radiolabeling is the high electronegativity of fluorine, which can drastically influence the physicochemical parameters and biological behaviour of a molecule in comparison to its unlabelled counterpart.

1.6 Radiofluorination methods

Various approaches for the introduction of a fluorine-18 radiolabel into a lead structure are known. Electron-rich reactants such as carbon-carbon double bonds, aromatic rings or carbanions can be labelled using electrophilic fluorination methods. Nucleophilic fluorination can be applied to electron-poor reactants such as substituted alkanes or aromatic structures with electron-drawing substituents.

1.6.1 Electrophilic fluorination

The source of fluorine for electrophilic fluorinations is [^{18}F]fluorine ([^{18}F]F_2) gas. It can be produced either by the ^{20}Ne (d, α) ^{18}F or ^{18}O (p,n)^{18}F reaction in a cyclotron. Milder, less reactive radiofluorination agents derived from [^{18}F]F_2 gas are acetylhypofluorite [^{18}F]CH_3COOF and xenon difluoride [^{18}F]XeF_2. [26, 27]

[^{18}F]F_2 cannot be produced carrier-free, since “cold” [^{19}F]F_2 gas needs to be introduced into the cyclotron target to remove ^{18}F adsorbed onto the target wall and to enable the formation of ^{18}F-^{19}F molecules. In this step, the radiofluorine adsorbed onto the target wall is recovered and an isotopic exchange takes place: a fluorine atom of [^{19}F]F_2 is exchanged for a fluorine-18 atom.

For this reason, every [^{18}F]F_2 molecule contains a ^{19}F atom. Theoretical specific acitivity is thus reduced to 50%. [17, 28]

Because of its high reactivity, the (regio-)selectivity of [^{18}F]fluorine is low. Formation of undesired side-products is regularly observed and makes extensive purification necessary. Often protective groups have to be introduced to protect reactive moieties, demanding further de-protection steps following the actual radiofluorination. [29]

Because of the disadvantageous properties of [^{18}F]fluorine and its derivatives, electrophilic fluorinations are used only if a simple nucleophilic route is not available and high specific activities are not necessary: e.g. when analogues of endogenous compounds present in the body in high concentrations – i.e. labelled sugars, amino acids or fatty acids [30] are used.

1.6.2 Nucleophilic fluorination

Nucleophilic substitution is performed using [^{18}F]fluoride as the fluorine source. It is available through the ^{18}O (p, n) ^{18}F reaction directly from the cyclotron. No-carrier-added (n.c.a.) [^{18}F]fluoride in high specific acivities is a mandatory prerequisite for the investigation of low-density receptor sites.

However, since [^{18}F]fluoride is obtained in an aqueous solution, it is highly hydrated and thus inactivated for nucleophilic substitution reactions. To activate [^{18}F]fluoride, it must be separated from its aqueous solution by means of an anion exchange resin and then transferred to the organic phase using a phase transfer catalysator.

Trace water is removed by azeotropic distillation with acetonitrile. This method is described in chapters 2.2.2. and 2.2.3. Since [^{18}F]fluoride is easily protonated to form [^{18}F]hydrofluoric acid ([^{18}F]HF), the reaction medium is basified to prevent protonation, which would make [^{18}F]fluoride unavailable for nucleophilic reactions. Nucleophilic substitution reactions take place in polar but aprotic solvents like acetonitrile, dimethyl sulfoxide (DMSO) or dimethyl formamide (DMF).

In terms of reaction mechanism, substitutions with [^{18}F]fluoride are displacement reactions of electron-drawing leaving groups like halides, tosylates, mesylates or triflate groups following a S_N2 mechanism.

An example for this type of reaction is the production of 2-[^{18}F]fluoro-2-deoxy-D-glucose ([^{18}F]FDG) from a fully acetylated mannose triflate precursor (1,3,4,6-tetra-O-acetyl-2-tnifluormethanesulfonyl-β-D-mannopyranose). [31] The triflate

group is displaced by the [^{18}F]fluoride ion. Subsequently, the protected hydroxy groups are de-protected by hydrolysis using acid or base, yielding [^{18}F]FDG. A scheme of this reaction is shown in Fig. 1.9.

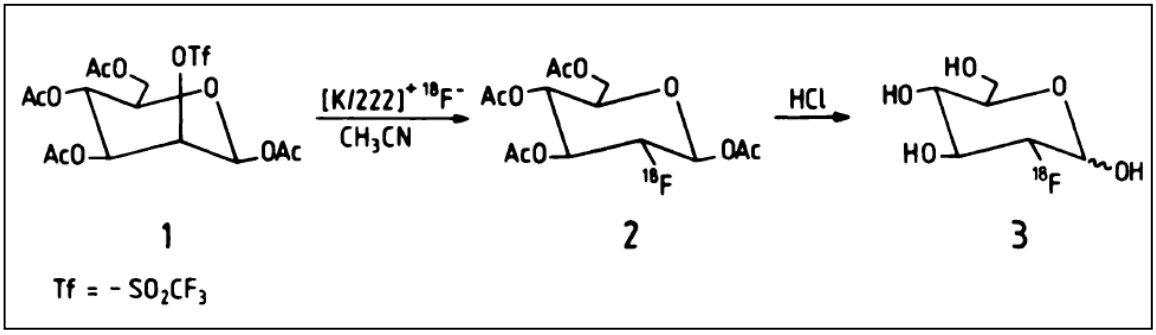

Fig. 1.9: Synthesis of [^{18}F]FDG from an acetylated mannose triflate precursor (from [24])

Nucleophilic fluorination of arenes is of great importance in the development of fluorine-18 labelled radiotracers because of the good metabolic stability of substituted aromatic compounds. [32]

To make arenes accessible to nucleophilic substitution reactions, they need to be activated by electron-drawing substituents in *ortho*- or *para*- position relative to the leaving group. Suitable leaving groups are nitro, cyano, carbonyl and especially trimethylammonium groups.

An example for this type of reaction is the one-step synthesis of [^{18}F]Altanserine from its *para*-substituted nitro-precursor and is shown in Fig.1.10.

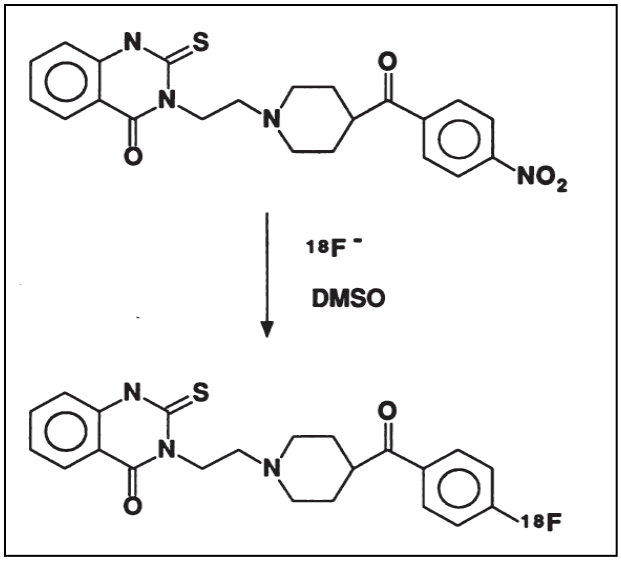

Fig. 1.10: Synthesis of [^{18}F]Altanserine in a one-step reaction (from [24])

1.7 Microfluidics in PET chemistry

Microfluidic chemistry is an approach to scale down chemical reactions from the mL to the µL range. Chemical synthesis on the micro-scale offers several advantages compared to conventional vessel-based chemistry. Since fluids in microstructures flow without turbulence, mixing can occur by diffusion only. The diffusional mixing resulting from laminar flow is very rapid. [33] The use of very small reaction volumes in the µL-range allows the usage of small amounts of precursor and radioactivity, leading to decreased formation of side products and reduced costs.

Since lower amounts of radioactivity are used, the radiation exposure of the operator is minimized. Another advantage of microfluidic systems is that most systems can be operated at high pressures (up to 400psi in the case of the Advion NanoTek LF ® system) so solvents can be used way above their boiling points at normal pressure. This enables the use of very high reaction temperatures impossible in vessel-based chemistry because of solvent evaporation occuring at room pressure.

The numerous advantages of microfluidic chemistry systems lead to higher incorporation yields, possibly lower amounts of side products and thus easier

product purification. It might even enable reactions that would not be possible under conventional radiolabelling conditions.

1.7.1 The Advion NanoTek LF

This integrated synthesis apparatus consists of a liquid flow (LF) reaction unit containing three microsyringe pumps for solvent / reagent transport and a reactor heater capable of holding up to four reactors. The coin-shaped microreactors are made of fused silica tubing held in a brass ring, which is filled with a thermoresistant polymer to hold the tubing in place.

All components of the system are accessed and controlled through a dedicated software interface. Reaction conditions (flow speed, reaction temperature, amounts of precursor and radioactivity used, time of residence in the reactor) were adjusted through this interface. All steps of the synthesis could be automated by using the proprietary programming language of the system.

It is also planned to connect the system to analytical instruments (e.g. HPLC and/or mass spectrometry) to constantly monitor the quality of the synthesized product and accordingly adjust reaction parameters.

The system is shown in Fig.1.11 with the liquid flow reaction module making up the biggest part of the system. The concentrator unit is shown in the far right of the picture. A more detailed schematic of the system set-up is shown in Fig. 2.4.

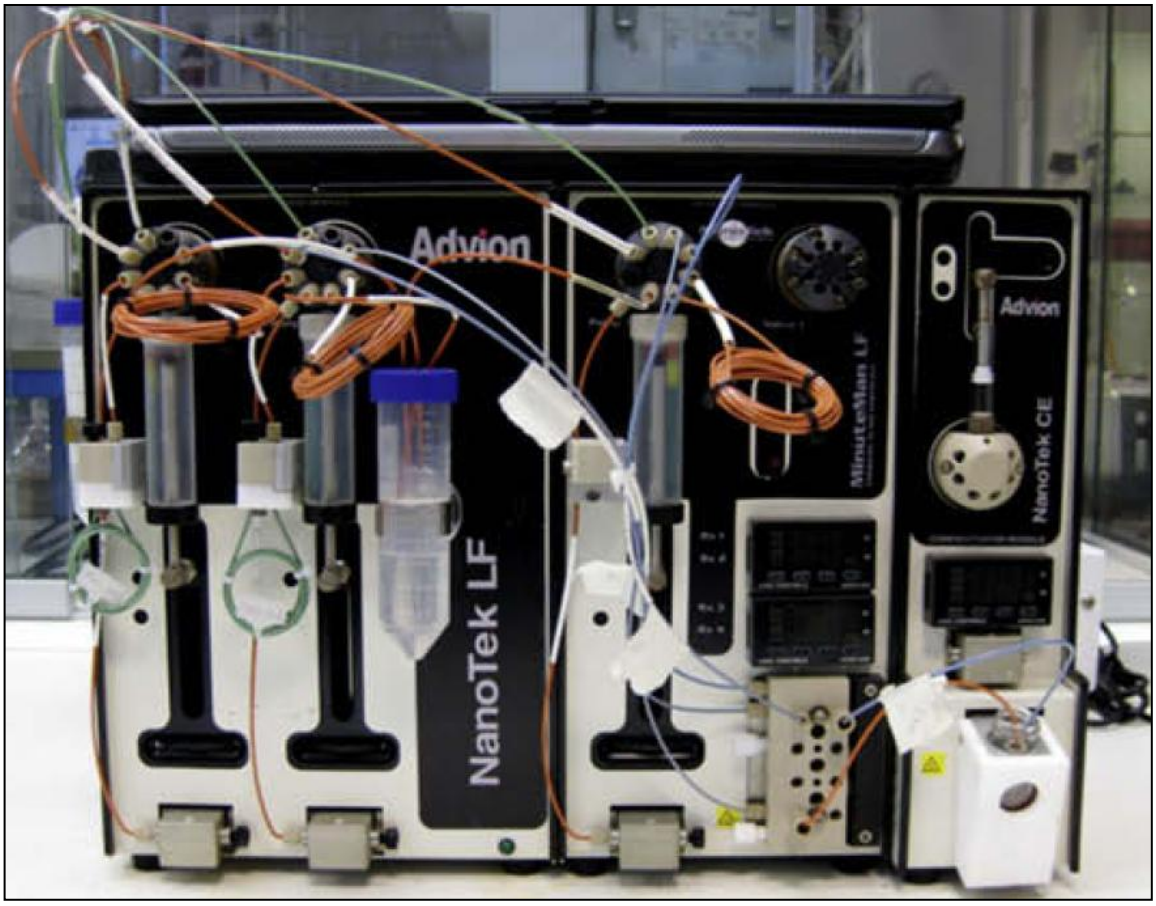

Fig. 1.11: The Advion NanoTek microfluidic chemistry system (from [34])

1.8 Dopamine

Dopamine (2-(3,4-Dihydroxyphenyl)ethylamine) is a biogenic amine of the group of catecholamines (derivatives of 1,2-dihydroxybenzene). It is biochemically synthesized from L-tyrosine. It was long thought to be only a precursor to epinephrine and norepinephrine, until Carlsson et al. discovered that dopamine is a neurotransmitter of its own in 1958. [35]

In the experiment leading to this discovery, male rabbits were injected with reserpine (an indole alkaloid from the roots of *Rauvolfia serpentina* that inhibits the vesicular monoamine transporter (VMAT-2) for 5-hydroxytryptamine (5-HT), dopamine (DA), epinephrine (E) and norepinephrine (NE). [36]

The result of reserpine treatment was a total depletion of catecholamines in the adrenal medullary as well as in other tissues, including the brain. The reserpine-treated animals were immobilized and sedated. (see Fig. 1.12)

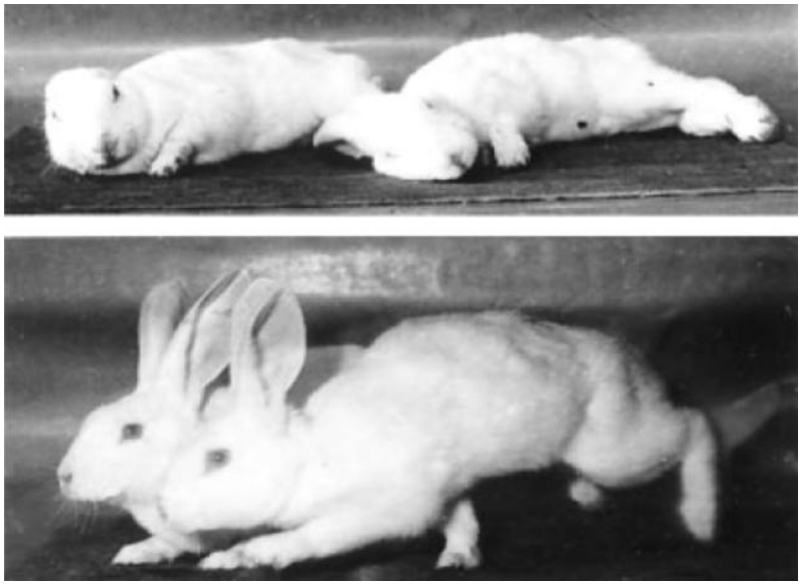

Fig. 1.12: Effects of L-DOPA on rabbits treated with reserpine (upper picture: reserpine-treated rabbits, lower picture: rabbits treated with L-DOPA following reserpine injection (from [37]))

Several hours after the injection of reserpine, the animals were treated with L-DOPA (the precursor of dopamine). 15 minutes after the L-DOPA injection the animals were "*instantaneously restored to full mobility and wakefulness by repletion of dopamine*". [35] When the researchers examined the brains of the animals, they found them still fully depleted of NE, but replenished of DA. Their conclusion was that dopamine must have restored the awareness and motor abilities of the reserpine-treated animals back to normal. [35]

This finding led the researchers to the assumption that dopamine plays a role other than that of a precursor to norepinephrine in brain physiology. This theory was even more strengthened by experiments indicating evidence of a "dopamine receptor" by Kebabian et al. in 1972 [38], leading to the discovery of the dopamine receptor subtypes D_1 and D_2 in 1979. [39] Further research in the 1980s revealed even more dopamine receptor subtypes.

1.8.1 Dopamine in human physiology

Dopamine plays an important role in many bodily functions. It is involved in the control of movement, motivation and cognition. [40] It is also considered a key substance in the development of reward-seeking behaviour. [41]

Dysfunctions of the dopaminergic system have implications in several neurologic and psychiatric diseases. Parkinson's disease, Chorea Huntington, schizophrenia and attention deficit hyperactivity disorder (ADHD) are the most prominent disorders linked to malfunctions of the dopaminergic system. [42]

1.8.1.1 Dopamine receptors

The physiological actions of dopamine are mediated through dopamine receptors. Structurally, all dopamine receptors consist of 7 transmembrane spanning helices, which can be divided into extracellular and intracellular sections. Dopamine binds to its extracellular binding pocket and initiates a conformational change of the receptor and a subsequent activation of the corresponding G-protein.

Based on sequence homology and pharmacology, dopamine receptors can be classified into two sub-families: the D_1-like receptors (D_{1A-1D} and D_5) and D_2-like receptors ($D_{2,3,4}$). [43] Receptors of the D_1-like family couple to G_s proteins which increase the activity of the adenylyl cyclase upon activation. Dopamine D_2-like receptors couple to G_i proteins which inhibit the activity of the adenylyl cyclase.

The modification of adenylyl cyclase activity through dopamine receptor activation leads to a change in the level of the second messenger cAMP (3',5'-cyclic adenosine monophosphate) and ultimately sets off a physiological response.

1.8.1.2 Dopaminergic pathways in the human brain

There are four major dopaminergic pathways in the central nervous system: the nigro-striatal, mesolimbic, mesocortical pathways and the tiberoinfundibular pathway. [44]

The axons of the nigro-striatal dopamine pathway project from the substantia nigra to the striatum. The nigro-striatal pathway is essential for motor regulation. When neurons in this pathway degenerate, symptoms of Parkinson's disease (tremor, rigidity and bradykinesia) develop.

The cell bodies of the mesolimbic and mesocortical dopamine pathway are located in the ventral tegmental area of the midbrain. They connect the ventral tegmental area to the limbic system, respectively the cortex.

The neurons of the mesolimbic dopamine pathway are activated when joy or desire are felt. [45] The behaviours connected with their activation are thereby reinforced. It has been shown that drugs of abuse promote dopamine release in the mesolimbic dopamine pathway. [45]

Lastly, the neurons of the tuberoinfundibular dopamine pathway project from the hypothalamus to the pituitary gland, where dopamine is involved in the regulation of prolactine secretion. [46]

1.8.1.3 Pathophysiology of the dopaminergic system

Abnormal dopaminergic transmission is present in several disorders of the CNS. The most prominent is Parkinson's disease. In Parkinson's, the degeneration of dopaminergic neurons in the nigro-striatal pathway causes the typical symptoms of this disease: tremor, rigidity and bradykinesia, as well as cognitive impairment. [47]

Another disease with impaired dopaminergic transmission is schizophrenia. Involvement of dopamine in schizophrenia has been first suggested by Van Rossum in 1967 in his dopamine hypothesis of schizophrenia. [48]

This theory was confirmed by Seeman et al. in 1975 in an experiment that verified that haloperidol, an antipsychotic, and dopamine bind to the same site in the brain, which was later found to be the dopamine D_2 receptor. [49] Through this discovery the involvement of the dopaminergic system in schizophrenia had clearly been proven.

Lastly, it has also been shown that the mesolimbic dopamine system plays an important role in the development of substance addiction. [41]

1.8.2 Imaging of the dopaminergic system

It is essential to have suitable radiotracers to study the role of the dopaminergic system in addiction, schizophrenia, Parkinson's disease and other diseases of the central nervous system. Several radiotracers, utilizing various types of radiolabels (^{99m}Tc, ^{123}I, ^{11}C and ^{18}F) have become available to study the components of the dopaminergic system using SPECT and PET imaging techniques. The targets of these radiotracers in the dopaminergic synapse are shown in Fig. 1.13 below.

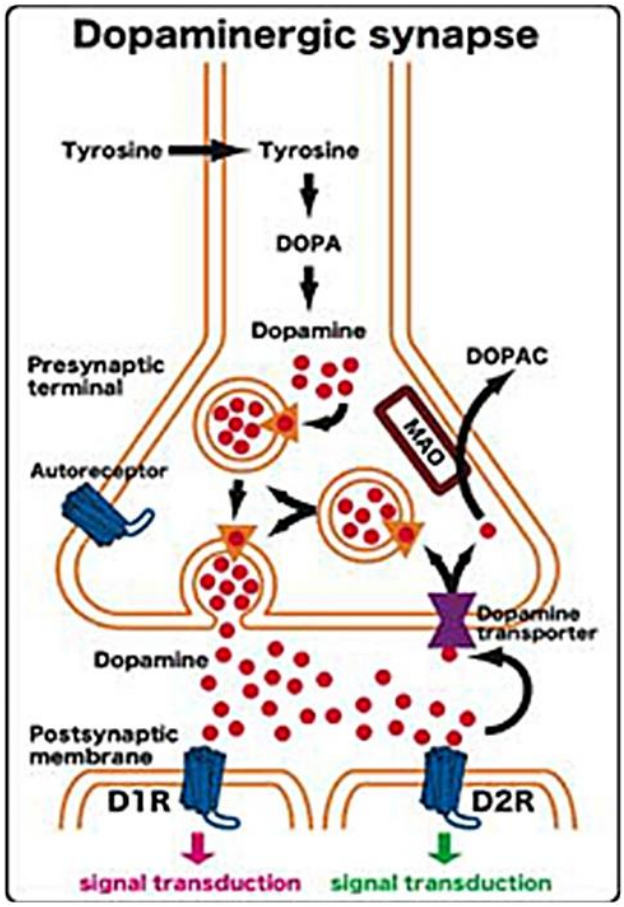

Fig. 1.13: Biochemistry of the dopaminergic synapse (from [50])

1.8.2.1 Imaging of the dopaminergic presynapse

The presynaptic components of the dopaminergic synapse include the dopamine reuptake transporter (DAT), enzymes of dopamine synthesis (DOPA decarboxylase), metabolism (MAO A, B) and the vesicular monoamine transporter (VMAT-2). A selection of radiotracers for SPECT and PET targeting these structures is shown in Table 1.4.

Since the abovementioned structures are unique to dopaminergic neurons, the binding of radiotracers strongly correlates with the number of intact dopaminergic neurons. Therefore, they can be used to estimate the number of remaining functional dopaminergic neurons in diseases of the basal ganglia. [51]

Dopamine synthesis and storage can be evaluated using 6-[^{18}F]fluoro-L-DOPA (FDOPA), which is actively transported across the blood brain barrier by an amino acid carrier, decarboxylated to [^{18}F]fluorodopamine and stored in vesicles analogously to endogenous dopamine. [52] The presynaptic dopamine reuptake transporter (DAT) can be targeted by radiotracers structurally similar to the DAT inhibitor (-)-Cocaine. The DAT is an important target in the diagnosis of early

Target	Name of tracer
Dopamine synthesis, storage	[^{18}F]FDOPA, [^{11}C]DOPA
Dopamine reuptake transporter (DAT)	[^{11}C]Nomifensin, [^{11}C]WIN, [^{99m}Tc]TRODAT, [^{123}I]β-CIT, [^{123}I]FP-CIT]
Vesicular monoamine transporter (VMAT-2)	[^{11}C]DTBZ
MAO B	[^{11}C]Deprenyl

Table 1.4: Tracer targets in the dopaminergic presynapse

stage Parkinson's disease when no motor signs are present yet, since binding to this transporter is a marker for the number of intact nigro-striatal dopaminergic

neurons. [53] A study has shown that decreased binding of [^{123}I]β-CIT to striatal DAT correlates to the severity of symptoms of the disease. [54]

As a further parameter of dopaminergic synapse function, the synaptic dopamine degradation rate by monoamine oxidase B (MAO B) can be assessed using a carbon-11-labelled MAO B inhibitor, [^{11}C]Deprenyl. [55]

1.8.2.2 Imaging of dopamine receptors

Dopamine receptors are present on both sides of the dopaminergic synapse (depicted in Fig.1.13). On the presynaptic side dopaminergic auto-receptors modulate the synthesis and release of dopamine while they function in cell-to-cell communication on the postsynaptic side. [56]

The first carbon-11-labelled dopamine D_1 antagonist was [^{11}C]SCH23390, a benzazepine derivative. It has been used to study the influence of age on dopamine D_1 receptor binding potentials. [57] Also, [^{11}C]SCH23390 has been used to assess the D_1 receptor occupancies in patients treated with a variety of antipsychotic drugs in order to investigate their sites of action [58].

Other uses of [^{11}C]SCH23390 were the assessment of D_1 receptor densities as a marker of brain degeneration in Huntington's disease [59, 60] and Parkinson's disease. [61]

Another dopamine D_1 receptor ligand possessing more favourable binding properties than [^{11}C]SCH23390 is [^{11}C]NNC112, also a benzazepine derivative. It shows lower accumulation in the cerebellum and higher affinity to dopamine D_1 receptors than [^{11}C]SCH23390. [62]

The synthesis of fluorinated benzazepine derivatives targeting the dopamine D_1 receptor has been described by Yang et al in [63]. This study has shown that the nitrogen atom of the azepine ring in substituted benzazepines cannot accommodate substituents larger than methyl without a significant loss of binding affinity.[63] Therefore, fluoroalkylations are not possible in this position. However, bulky substituents can be tolerated in the phenyl ring in all positions without a

significant loss of binding affinity. [64] A fluorinated benzazepine D_1 receptor tracer is shown among two carbon-11 labelled benzazepines in Fig. 1.14.

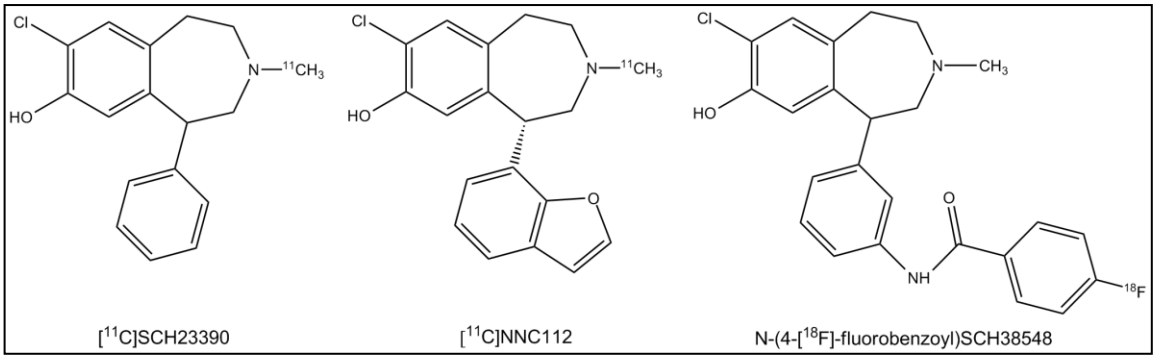

Fig. 1.14: Structures of ^{11}C and ^{18}F- labelled dopamine D_1 receptor tracers (from [63])

The dopamine D_2 receptor is the main target for classic neuroleptics. Therefore, several dopamine D_2 receptor radiotracers have been used to assess the relationship between D_2 receptor occupancy and therapeutic efficacy of neuroleptics. [65]

The lead structure for dopamine D_2 receptors are the substituted benzamides. First-generation benzamide radiotracers, [^{11}C]Raclopride and [^{123}I]IBZM, exhibited only moderate affinities for the D_2 receptor. For this reason, imaging of D_2 receptors was possible only in a brain area with very high dopamine D_2 receptor density, namely the striatum.

Recently developed high-affinity D_2 receptor tracers such as [^{11}C]FLB457 and [^{18}F]Fallypride allow the imaging of dopamine D_2 receptors also in extrastriatal brain areas, where the concentration of D_2 receptors can be up to two orders of magnitude lower than in the striatum. [66]

With these ligands, the binding of antipsychotic drugs to extrastriatal D_2 receptors can be investigated and new insights into the role of these receptors in neuropsychiatric disorders can be gained. [67]

1.8.2.3 Imaging of dopamine D_2 receptors using [^{18}F]Fallypride

Mukherjee et al. developed the dopamine D_2 tracer [^{18}F]FPMB in 1990. Because of its moderate lipophilicity (log K_w = 1.64), the brain uptake of [^{18}F]FPMB in cebus monkeys was limited to 0.06% per injected dose. [68]

For this reason, the N-ethyl group in [^{18}F]FPMB was substituted for a N-allyl group, leading to the compound [^{18}F]Fallypride. This compound showed improved lipophilicity (log K_w = 2.43) and brain uptake (0.10% per injected dose). Also, an increased affinity for D_2-like receptors (K_i = 0.03nM for [^{18}F]Fallypride versus K_i = 0.26nM for [^{18}F]FPMB) [69] has been observed.

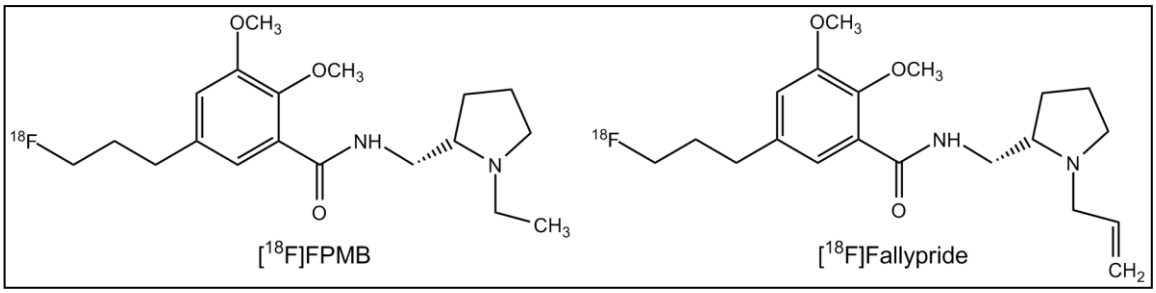

Fig. 1.15: Structures of the dopamine D_2 receptor tracers [^{18}F]FPMB and [^{18}F]Fallypride

Biodistribution studies in rats have shown rapid clearance of [^{18}F]Fallypride from unspecific binding sites like cerebellum and frontal cortex and preferential binding of [^{18}F]Fallypride to striatal receptors. A striata-to-cerebellum rate of 122 was observed 2 hours post-injection [69], which is higher than previously observed with fluorine-18-labelled substituted benzamides and salicylamides [70]

[^{18}F]Fallypride has been used to assess dopamine $D_{2/3}$ receptor distribution in humans, showing accumulation of radioactivity in striatal and extrastriatal regions. [71]

Another interesting study conducted with [^{18}F]Fallypride was the measurement of dopamine release mediated by *d*-amphetamine. Riccardi et al. found a significant decrease in [^{18}F]Fallypride binding potentials in various brain regions, indicating amphetamine-mediated stimulation of dopamine release in these regions. [72]

[^{18}F]Fallypride has also been used to quantify dopamine D_2 receptor occupation by the atypical antipsychotic clozapine in schizophrenic patients. This examination by Grunder et al. showed that clozapine primarily binds to extrastriatal D_2 receptors in the cortex, which may explain the lower incidence of extrapyramidal symptoms in the class of atypical neuroleptics, to which clozapine belongs. [73]

The comparison of receptor binding potentials in healthy volunteers and clozapine-treated schizophrenics can be seen in Fig. 1.16.

In summary, [^{18}F]Fallypride has several advantages in comparison to older dopamine D_2 receptor tracers, including its increased lipophilicity and higher affinity to dopamine D_2-like receptors. These improved characteristics allow the visualization of dopamine D_2-like receptors in brain areas with low dopamine D_2-like receptor densities.

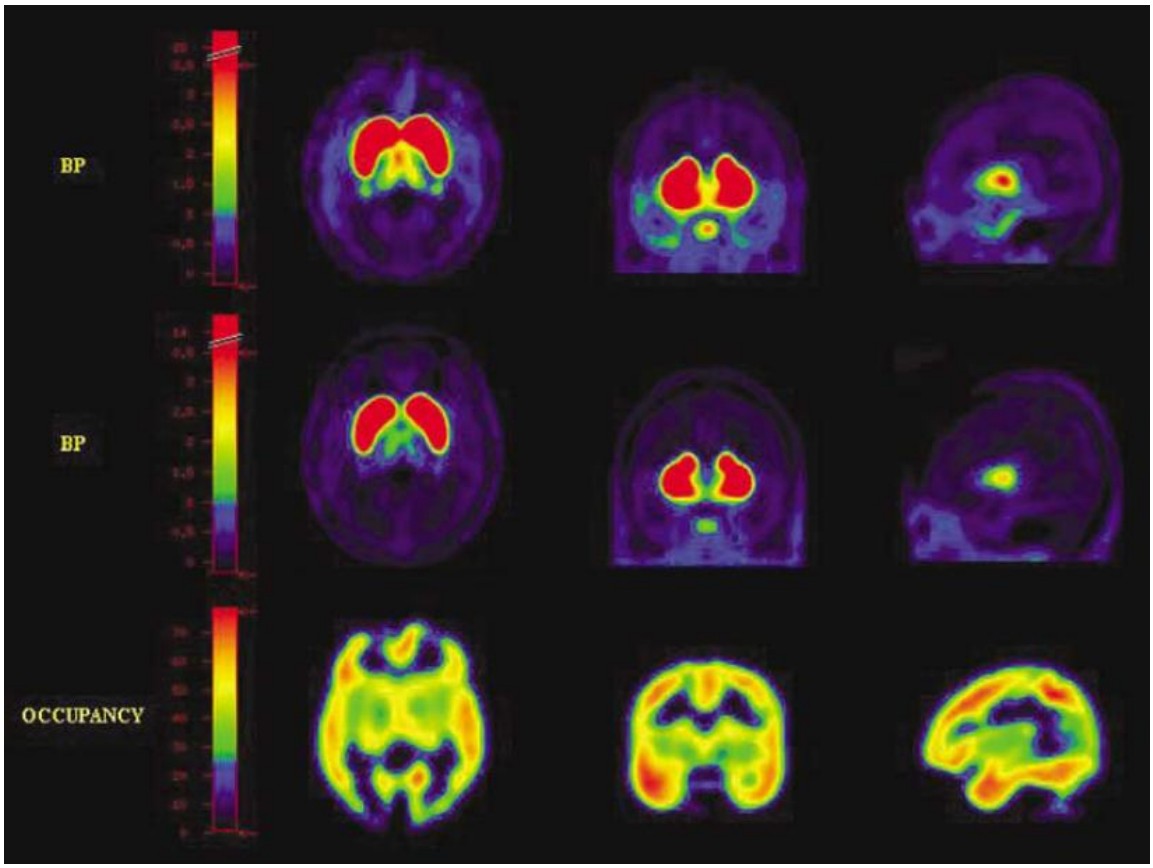

Fig. 1.16: Mean binding potentials of dopamine D_2-like receptors in healthy volunteers (top row) and clozapine-treated schizophrenics (middle row), measured with [^{18}F]Fallypride PET. The D_2/D_3 receptor occupancy distribution is shown in the bottom row. (from [73])

2 Materials and methods

2.1 Materials

All chemicals were used as bought if not stated otherwise.

2.1.1 Synthesis chemicals

- Precursor: (S)-2,3-dimethoxy-5-[3-[[(4-methylphenyl)-sulfonyl]oxy]-propyl]-N-[[1-(2-propenyl)-2-pyrrolidinyl]methyl]benzamide was purchased from ABX-Advanced Biochemical Compounds. (Dresden, Germany)
- Reference standard: 5-(3-fluoropropyl)-2,3-dimethoxy-N-[[(2S)-1-(2-propenyl)-2-pyrrolidinyl]methyl]benzamide was purchased from ABX-Advanced Biochemical Compounds.

2.1.2 Solvents, buffers

- Acetonitrile and ammonium formate were bought from Merck (Darmstadt, Germany).

2.1.3 TLC and HPLC equipment

- Analytical thin layer chromatography (TLC) was performed on Silicagel RP-18 60 F_{254} plates from Merck.
- HPLC analyses were performed on a Merck LiChrospher 100-250 RP-18e column (5µm, 250mm x 4.6mm) using a Merck-Hitachi LaChrom gradient system being comprised of a L-6200 gradient pump, a Merck-Hitachi L-7400 UV detector set to a wavelength of 254nm and a lead-shielded NaI radiodetector by Berthold Technologies.(Bad Wildbad, Germany)
- Autoradiographic analyses of TLC plates were performed on an InstantImager apparatus from Packard Instrument Company.(Meriden, USA)

2.1.4 Cyclotron equipment

- [^{18}F]Fluoride was produced using the ^{18}O(p, n)^{18}F nuclear reaction in a GE PETtrace cyclotron (16.5 MeV protons).

- Enriched $H_2{}^{18}O$ was bought from Rotem Medical.(Dimona, Israel)

2.1.5 Phase transfer of [^{18}F]Fluoride

- Kryptofix 2.2.2. (4,7,13,16,21,24-Hexaoxa-1,10-diazabicyclo[8.8.8]-hexacosane) and K_2CO_3 were bought from Merck.
- Elution of [^{18}F] was accomplished using Chromafix® 30 PS-HCO_3 cartridges (Macherey-Nagel, Düren, Germany).

2.1.6 Vessel based synthesis

- Vessel based syntheses were performed in 1mL Grad V-Vials with 13-425 S/T Caps from Wheaton Science Products. (Millville, USA)
- Vials were sealed with PTFE silicone septa from Wheaton Science Products.

2.1.7 Microfluidic synthesis apparatus

- Microfluidic syntheses were performed on a NanoTek LF Microfluidic synthesis apparatus from Advion BioSystems. (Ithaca, USA)
- Azeotropic drying for the microfluidic syntheses was performed in the NanoTek CE Unit from Advion BioSystems.
- The system was operated using a Laptop computer with the NanoTek LF 3.2 software installed.

2.2 Methods

2.2.1 Production of [^{18}F] F^- in the GE PETtrace cyclotron

[^{18}F]fluoride was produced by irradiation of [^{18}O]water (>98%) with a proton beam, utilizing the ^{18}O (p, n)^{18}F nuclear reaction in a silver target.

The irradiation process and product delivery were controlled by a computer module. When the desired activity level was reached, irradiation was stopped and the product was delivered into a V-vial situated in a lead-shielded hot cell.

Because the [^{18}F]fluoride was delivered in a solution of [^{18}O]water, further steps were necessary to make it available for nucleophilic substitution reactions in organic solvents.

2.2.2 Complexation, phase transfer and azeotropic drying of [^{18}F]Fluoride

The removal of bulk [^{18}O]water was achieved by passing the aqueous [^{18}F]fluoride solution through an anion exchange cartridge. The [^{18}F]fluoride was thereby retained on the cartridge while the [^{18}O]water was collected seperately.

Subsequently, the cartridge was eluted with 1mL of a solution of potassium carbonate (4.5mg, 32.6µmol) and the cryptand Kryptofix 2.2.2. (20mg, 53.2µmol) in acetonitrile / water (70:30 v/v%).

The potassium cation is complexed by the aminopolyether Kryptofix 2.2.2. As the counter-ion of the complexed K^+, [^{18}F]fluoride is dragged into the organic phase together with the potassium-Kryptofix 2.2.2. complex, leaving a highly activated [^{18}F]fluoride ion.

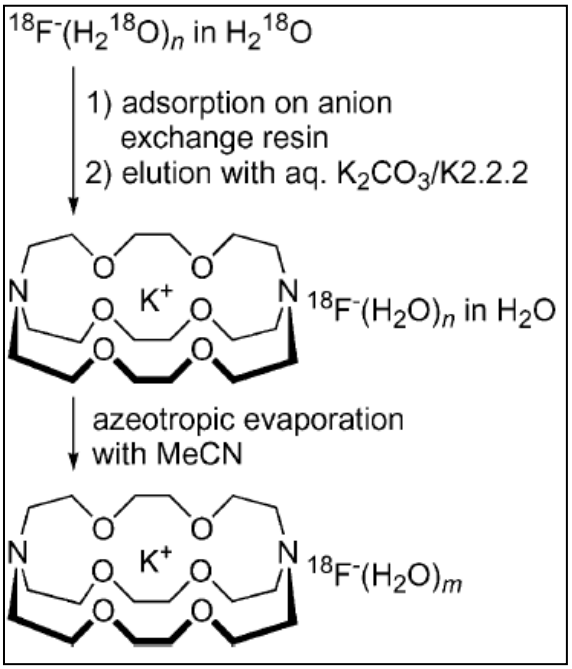

Fig. 2.1: Complexation and phase transfer of [^{18}F]fluoride (from [74])

To ensure sufficient nucleophilicity for nucleophilic substitution reactions, [^{18}F]fluoride had to be stripped of hydrate water (up to 15 [^{18}O]water molecules can surround a fully hydrated $^{18}F^-$ ion). [75]

Water and acetonitrile form a minimum boiling point azeotrope (83.7% acetonitrile (w/w)) boiling at 76.5°C at atmospheric pressure [76]. For this reason, water can be easily removed by evaporating the solution to dryness.

Thus, the solution was heated to 100°C and trace water was azeotropically removed by adding 3 portions of acetonitrile (each 250µL) over a course of 15 minutes. This process was carried out under a stream of nitrogen gas.

The dried [^{18}F]fluoride was then dissolved in anhydrous acetonitrile and transferred to the reaction vessels.

2.2.3 Synthetic route

The synthesis of (S)-N-[(1-allyl-2-pyrrolidinyl)methyl]-5-(3-[^{18}F]fluoropropyl)-2,3-dimethoxybenzamide, abbreviated [^{18}F]Fallypride, started from the precursor substance *(S)-N*-[(1-allyl-2-pyrrolidinyl)methyl]-5-(3-tosyloxypropyl)-2,3-dimethoxybenzamide, abbreviated tosyl-Fallypride. It was carried out as a one-step synthesis by adding a solution of the [^{18}F]fluoride-K2.2.2-K^+-complex to the precursor solution. The solvent in both synthesis techniques was acetonitrile.

The mechanism for the introduction of the radiolabel was the nucleophilic substitution of the toluenesulfonic acid group in the precursor substance by [^{18}F]fluoride.

This reaction yields [^{18}F]Fallypride and the resonance-stabilized toluenesulfonic acid anion as the leaving group. Since the negative charge is delocalized throughout the leaving molecule, it makes an excellent leaving group by not competing as a nucleophile with [^{18}F]fluoride. A schematic of the reaction is depicted in Fig. 2.2.

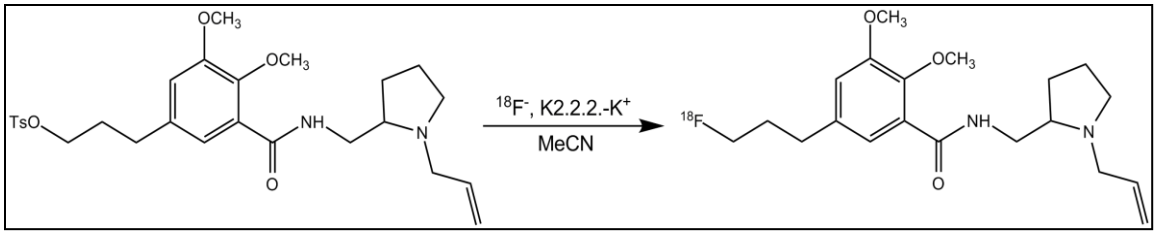

Fig. 2.2: Synthetic route of the radiofluorination of tosyl-Fallypride

2.2.4 Vessel-based synthesis of [^{18}F]Fallypride

Vessel-based synthesis of [^{18}F]Fallypride was carried out by adding a solution of the dry n.c.a. [^{18}F]fluoride-K2.2.2-K^+-complex to a solution of tosyl-Fallypride dissolved in acetonitrile. The reaction took place in 1mL V-Vials which were sealed with septa and then placed in an aluminum heating block for the specified period of time. Immediately after completion, reaction mixtures were analyzed for determination of radiochemical incorporation yields and impurities using radio-TLC and radio-HPLC.

The influence of reaction temperature on synthesis yields was tested at 40°C, 60°C, 70°C, 80°C and 85°C using a fixed precursor concentration of 5mg/mL and a fixed reaction duration of 15 minutes. Since these reactions were carried out under room pressure, higher temperatures could not be evaluated because of the boiling point of the solvent acetonitrile.

The influence of precursor concentration and reaction duration on reaction yields was evaluated. Precursor concentrations used were 1mg/mL, 2.5mg/mL and 5mg/mL. These experiments were carried out at varying reaction times of 2, 5, 15 and 30 minutes while the reaction temperature was held constant at 70°C.

2.2.5 Microfluidic synthesis of [^{18}F]Fallypride

The microfluidic synthesis of [^{18}F]Fallypride was carried out using the Advion NanoTek LF microfluidic synthesis apparatus as described in chapter 1.7.1. A detailed schematic of the system set-up is presented in Fig 2.3.

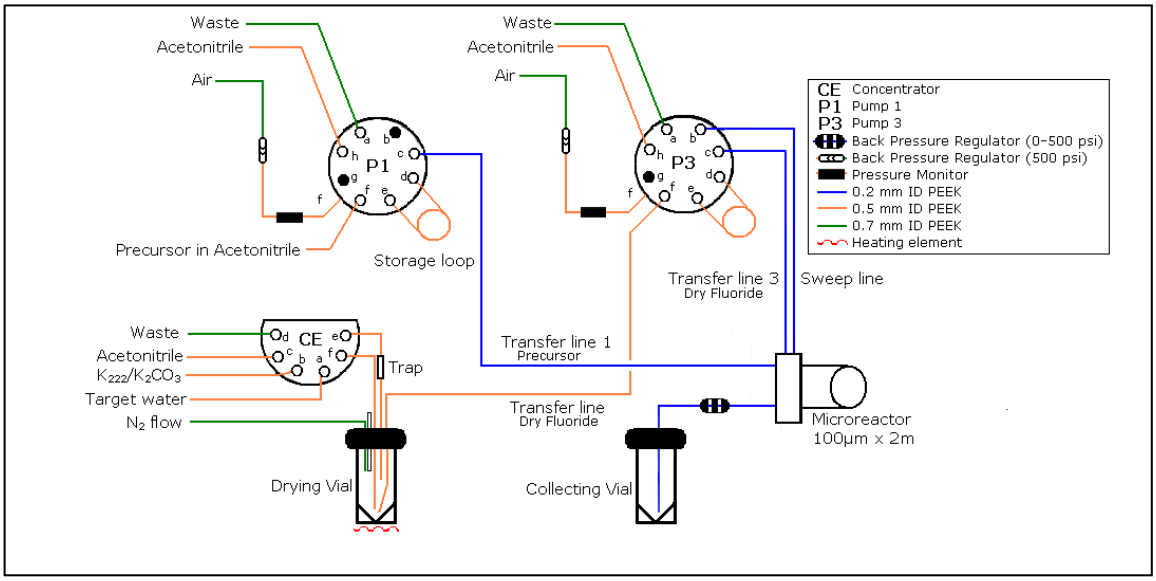

Fig. 2.3: Schematic illustration of the set-up of the Advion NanoTek LF system (from[77])

Before a series of experiments was started, all components of the system were flushed with purified water and acetonitrile in order to remove any potential contaminations present in the system. Cleaning runs were fully automated by using a macro written in the proprietary programming language of the Advion NanoTek LF system. The source code of the master cleaning routine for reagent lines, solvent and waste lines, storage loops, magnetic valves and the microreactor is shown in Fig. 2.4.

Time delay	Pump Action	Comment
0	/7o6R	Valve F
0	/1L3702000000004C□□L360200025005 2□	Concentrator Temp 20
0	/1L3502000020004C□	reactor4 temp 20
0	/1L3402000020004B□	reactor3 temp 20
0	/1L3302000020004A□	reactor2 temp20
0	/1L3202000025004E□	reactor1 temp20
0	/1o1V10000A0o8V10000A48000o1V10000A0o8V1600A48000R	2x P1 leeren, mit LM fuellen
0	/2o1V10000A0o8V10000A48000o1V10000A0o8V1600A0o8V1600A48000R	2x P2 leeren , mit LM fuellen
0	/3o1V4000A0o8V4000A48000o1V8000A0o8V800A48000R	2x P3 leeren, mit LM fuellen
100000	/1o3V64A28800R	P1: Port C mit 200uL spuelen 40mL/min
0	/2o3V64A28800R	P2: PortC mit 200uL spuelen 40mL/min
0	/3o4V160A9600o6V160A0R	P3: Port D (loop ueber reagent line) 800uL: 200uL/min; Port F 200uL: 200uL/min
310000	/1o8V1600A48000o4V160A0R	P1: Syringe fill; port D 500uL: 100uL/min
0	/2o8V1600A48000o4V160A0R	P2: syringe fill; port D 500uL: 10uL/min
0	/3o8V800A48000o5gv700D1M10G14400o2gv700D1M10G14400R	P3: fill syringe; portE-D-C 300uL: 50uL/min; portB 300uL: 50mL/minP3 Move

Fig. 2.4: Commented source code of the master cleaning routine for the Advion NanoTek LF system.

After the initial cleaning run, the preparation of [^{18}F]fluoride from target water started. Also for this process, a macro was programmed to fully automate the separation and azeotropic drying of [^{18}F]fluoride. (see Fig. 2.5)

The [^{18}F]fluoride anion was separated from the solution of [^{18}O]water by trapping it on an anion exchange cartridge (PS-HCO_3) and subsequent elution from the cartridge with a solution of Kryptofix 2.2.2 (20mg, 53.2µmol) and potassium carbonate (4.5mg, 32.6 µmol) in acetonitrile/water (70:30 v/v%). Removal of residual water was performed by azeotropic drying of the resulting solution.

In the drying process, 500µL acetonitrile from the pump of the CE unit and two 200µL portions from pump 3 of the LF unit were added over a course of 15 minutes. After completion of the drying process, the dried [^{18}F]fluoride was re-solved in 500µL acetonitrile.

Time delay	Pump Action	Comment
0	Wait	Batch FDG: SBFDG_v35; Plumbing: SBFDGv2_1 ; 3-Channel Reactor; 500 uL run, ;N2 Flow set to 1.5 scfh
0	/3o8V4000A48000R	P3 : fill syringe
0	L3702000100004DL3602000300004E	Heat concentrator 1 up to 100 C
1000	/5go1V3200A12000M2000o5V1200A0M500G3go6V6400A12000M1000o1A0G4R	CE: Load Target Water
120000	/7U2M5000U1M5000u2R	G: Turn on Nitrogen
20000	/5o2V2400A6000o5V2400A0R	CE: add 0,5mL K222
10000	/5o3V2000A6000M2000o5V75D4800o6V75D1200o2V2000A0R	CE: Add 0.5 mL MeCN
10000	L3702000110004EL3602000300004E	Heat concentrator 1 up to 110C
200000	/3o6V10000D9600R	P3: add 200uL MeCN
60000	/3o6V10000D9600R	P3: add 200uL MeCN
50000	L37020000260054L3602000300004E	CE: Set Heater to 26oC
300000	/7u1R	G: Turn off Nitrogen
1000	/3o6V10000D24000R	P3: solve Activity in 500uL MeCN

Fig. 2.5: Commented source code of the azeotropic drying routine for [^{18}F]fluoride.

The precursor solution containing tosyl-Fallypride and dry [^{18}F]fluoride were then loaded into the storage loops of pump 1 and 3 of the LF unit. Transfer lines 1 and 3 were filled with the respective solutions from loop 1 and 3 and the reactor was swept with acetonitrile via pump 3.

After the preparatory steps described above, the system was ready to perform reactions. In the reaction depicted in Fig. 2.6, 30µL of dried [^{18}F]fluoride solution and 30µL of precursor solution were pushed through the reactor at an overall flow rate of 60µL/min. The subsequent sweep 1 performed via pump 3 pushed the reaction mixture out of the system. The final sweep cleaned the system of

remaining reactands and pushed the reaction mixture into the collecting vial. The total reaction volume was 100µL of reaction mixture + 15.7µL for sweep 1 + 20µL to the distribution valve + 300µL to the collecting vial, adding up to 335.7µL of total reaction volume. The duration for a single experiment was 289 sec.

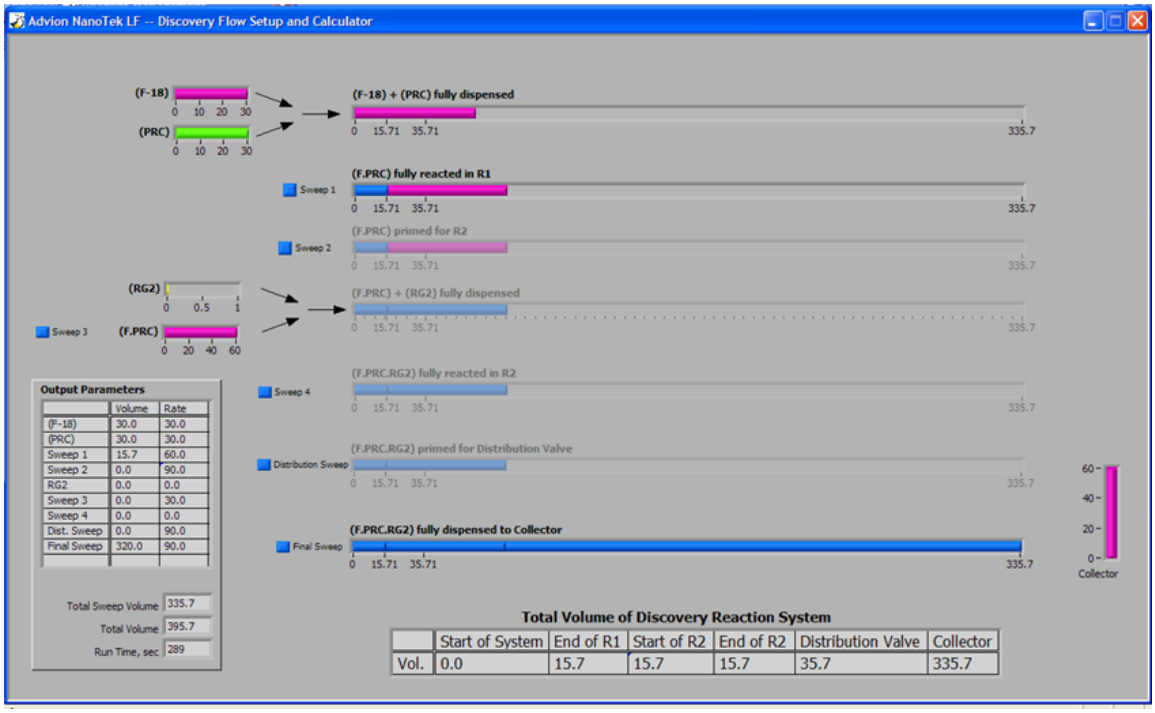

Fig. 2.6: The course of events in a typical reaction using the discovery mode of the Advion NanoTek LF

An additional tool for reaction control was the pump pressure and radiation graph. The system possesses three built-in pressure sensors that transmit the pressure status of every pump to the user interface.

The system also comes with three radiation detectors that can be placed freely at any spot of the system. A radiation sensor was placed on the storage loop for the [^{18}F]fluoride solution to monitor the decay of [^{18}F]fluoride during a series of experiments.

The data collected from the pressure and radiation sensors were recorded in a real-time graph visible in the main window of the user interface. The graph for the discussed reaction is shown in Fig. 2.7.

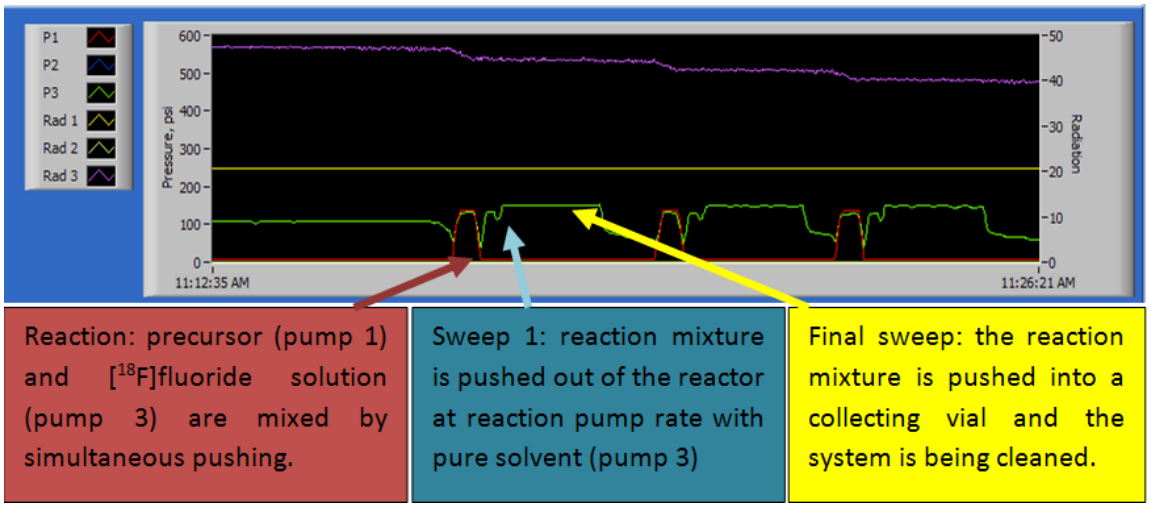

Fig. 2.7: Detector graph for a triplet experiment of the reaction shown in Fig. 2.6. Graphs P1, P2, P3 represent the pressure course of the particular pump. Rad1, Rad2, Rad3 represent radiation detectors.

The influence of reaction temperature and precursor concentration on synthesis yields was evaluated at room temperature (26°C), 100°C, 140°C, 150°C, 160°C, 170°C and 180°C for precursor concentrations of 0.5mg/mL 1mg/mL, 2.5mg/mL and 5mg/mL. All reaction temperatures were evaluated in a series of experiments for each precursor concentration.

2.2.6 Quality control procedures

To ascertain the purity of the resulting [^{18}F]Fallypride and to evaluate the radiochemical yields of a reaction, a quality control system was set up. A radio-TLC system was used for the quantification of radiochemical incorporation yields and determination of potential side-products. The identity of the reaction products and side-products was evaluated using a radio-HPLC assay.

2.2.6.1 Development of a thin layer chromatography system for the autoradiographic quantification of [^{18}F]Fallypride

To achieve sufficient separation of the reaction product from unreacted [^{18}F]fluoride and side-products at short running times, several TLC systems were evaluated. Stationary phases used were silica gel 60 F_{254} and silica gel 60 RP-18 F_{254S}.

Abbreviation	Composition of the eluent
A	95/5 MeCN / H_2O (v/v%)
B	90/10 MeCN / H_2O (v/v%)
C	80/20 MeCN / H_2O (v/v%)
D	70/30 MeCN / H_2O (v/v%)
E	60/40 MeCN/ H_2O (v/v%)
F	80/20 MeOH / H_2O (v/v%)
G	50/50 MeOH / 1M Ammonium acetate buffer (v/v%)

Table 2.1: Compositions of eluents used in radio-TLC

The separation of unreacted [^{18}F]fluoride from the product was the most important factor for the usability of a chromatographic system. A prerequisite for a usable TLC system was the fixation of [^{18}F]fluoride at the starting point of the TLC run. This precondition was not fulfilled by eluents containing higher amounts of water (eluents D, E, F, G) as these were able to solve and transport the [^{18}F]fluoride ion. Details concerning the evaluation of R_F values of [^{18}F]fluoride and [^{18}F]Fallypride using the eluents listed in table 4 are presented in Table 2.2.

Also, when silica gel 60 phases were used in combination with an eluent containing a high percentage of water, intense smearing of the substance over a wide R_F range was observed. We were able to avoid smearing by using a RP-18 stationary phase with a high percentage of non-polar solvent in the mobile phase instead. (eluents A, B or C)

Best results were obtained using silica gel 60 RP-18 F_{254S} and eluent A (95% acetonitrile / 5% water v/v%) because of sufficient separating capacity, concise peak form and short run times of this chromatographic system.

The result of a TLC separation using silica 60 RP-18 F_{254S} plates as a stationary phase and eluent A as the mobile phase is presented in Fig. 2.8. The unreacted [^{18}F]fluoride was retained at the starting point while [^{18}F]Fallypride was

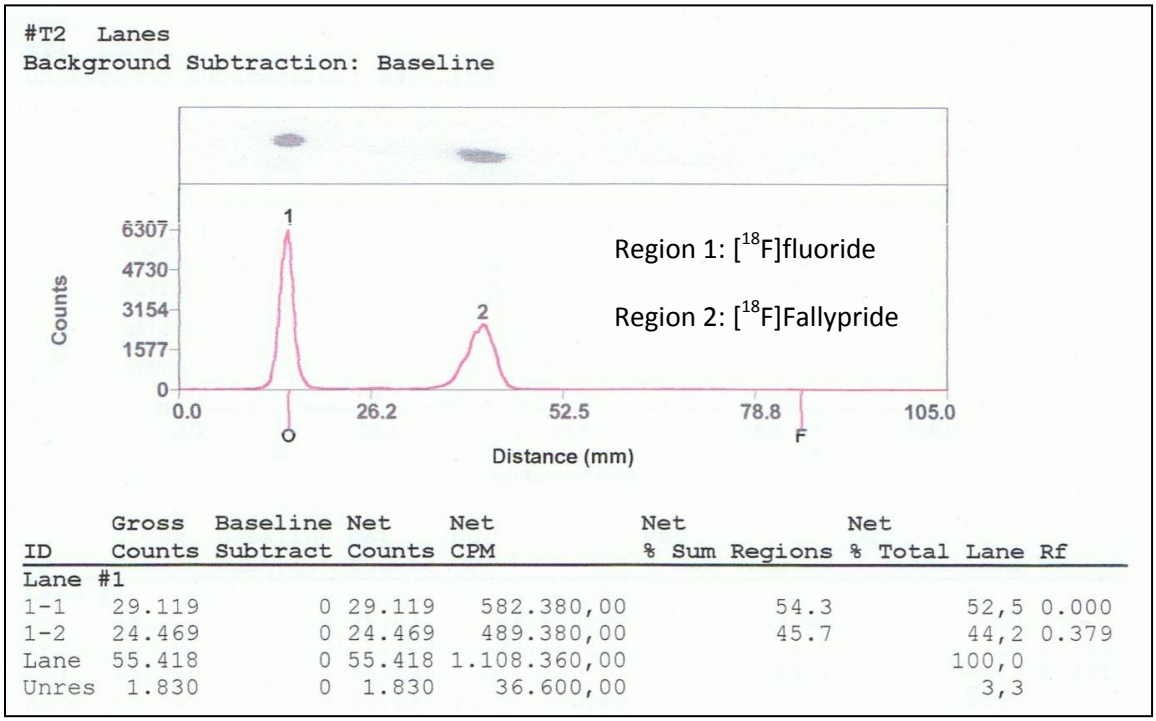

ID	Gross Counts	Baseline Subtract	Net Counts	Net CPM	Net % Sum Regions	Net % Total	Lane Rf
Lane #1							
1-1	29.119	0	29.119	582.380,00	54.3	52,5	0.000
1-2	24.469	0	24.469	489.380,00	45.7	44,2	0.379
Lane	55.418	0	55.418	1.108.360,00		100,0	
Unres	1.830	0	1.830	36.600,00		3,3	

Fig. 2.8: Results of the separation of [^{18}F]Fluoride from [^{18}F]Fallypride using radio-TLC. [^{18}F]fluoride remains at the starting point.

transported by the eluent, leading to separation of both substances. The radioactive spots on the TLC strips were quantified using an InstantImager autoradiographer, allowing the determination of radiochemical incorporation yields of reactions.

In Table 2.2, R_F values of TLC runs with [^{18}F]fluoride or [^{18}F]Fallypride using various combinations of mobile and stationary phases are presented. When two values are listed for a substance, the substance peak has been split up during the separation run, making the TLC system unusable for separation runs.

Eluent	$[^{18}F]F^-$ in a solution of H_2O (R_F)		Product solution (R_F)	
	KGF_{254}	RP-18	KGF_{254}	RP-18
A 95/5 (v/v) MeCN / H_2O	0.006±0.0005	0.042±0.035	0.441±0.031	0.377±0.056
B 90 /10 (v/v) MeCN / H_2O	0.002±0.004	0.002±0.003	0.417±0.011	0.573±0.050
C 80/20 (v/v) MeCN / H_2O	0.029±0.009	0.012±0.013	0.791±0.013	0.708±0.023
D 70/30 (v/v) MeCN / H_2O	0.066±0.013	0(5.15%) / 0.1575±0.006 (91.7%)	0.823±0.018	0.769±0.009
E 60/40 (v/v) MeCN / H_2O	0.038±0.061 (5.7%) / 0.377±0.004 (91.10%)	0 (2.03%) / 0.5803±0.010 (96.53%)	0.834±0.039	0.848±0.066
F 80 / 20 (v/v) MeOH / H_2O	0 (8.35%) / 0.195±0.0037 (88.2%)	0 (4.07%) / 0.567±0.104 (93.8%)	no separation	no separation
G 50/50 (v/v) MeOH/ 1M Ammonium acetate buffer	0.147±0.049	0.271±0.062	no separation	no separation

Table 2.2: Development of a TLC system for the separation of $[^{18}F]$fluoride from $[^{18}F]$Fallypride (n ≥ 2).

2.2.6.2 Development of a radio-HPLC system for the identification of [^{18}F]Fallypride and possible by-products.

Radio-HPLC was performed on a LiChrospher 100-250 RP-18e column (5µm, 250mm x 4.6mm). 20µL of the reaction mixture were injected into the HPLC system and separated using a gradient of acetonitrile (=eluent A) and 25mM ammonium formate buffer. (=eluent B) The gradient started at 40% A and was gradually increased to 60% A from minute 5 to 6. It was then kept at 60% A until minute 12. The column was re-equilibrated for 3 minutes to 40% A before starting the next HPLC analysis. The radioactive components of the reaction solution were detected using a NaI scintillation detector, while non-radiactive components were detected using a standard UV detector adjusted to a wavelength of 254nm.

Due to its hydrophilicity, the [^{18}F]fluoride ion was hardly retained and eluted almost immediately after injection into the column. (t_R = 1.02 minutes). [^{18}F]Fallypride and the internal standard [^{19}F]Fallypride eluted at t_R=7.45 respectively t_R = 7.48 minutes while the precursor tosyl-Fallypride eluted at t_R = 11.00 minutes.

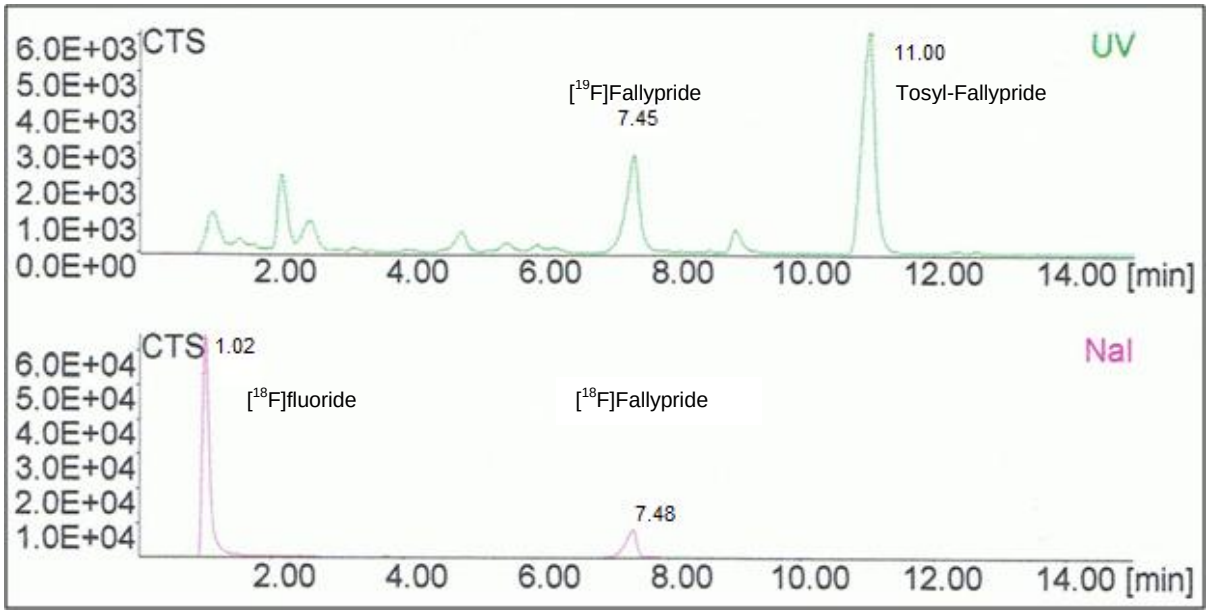

Fig. 2.9: Sample chromatogram of the separation of [^{18}F]Fluoride from [^{18}F]Fallypride by radio-HPLC

3 Results

All results are presented as decay-corrected radiochemical incorporation yields (RCIYs).

3.1 Vessel-based synthesis of [^{18}F]Fallypride

A distinct dependency upon increasing reaction temperature was observed. Only little conversion (4.9±1.0%) was observed at 40°C for reactions at 5mg/mL precursor concentration in reaction mixture and 15min reaction duration.

Highest radiochemical incorporation yields were achieved at 85°C (54±7%). Because the boiling point of acetonitrile is 81.6°C at atmospheric pressure, reactions conducted at this temperature were at risk of solvent evaporation. (see high standard deviations above 70°C)

Reaction temperature (°C)	Total mean yield (%)	Standard deviation (%)
40°C	4.9	1.0
60°C	24.8	1.5
70°C	36.1	12.5
80°C	43.6	7.3
85°C	54.3	7.0

Table 3.1: Dependency of reaction yields upon reaction temperature at a constant precursor concentration of 5mg/mL, stirred for 15 minutes

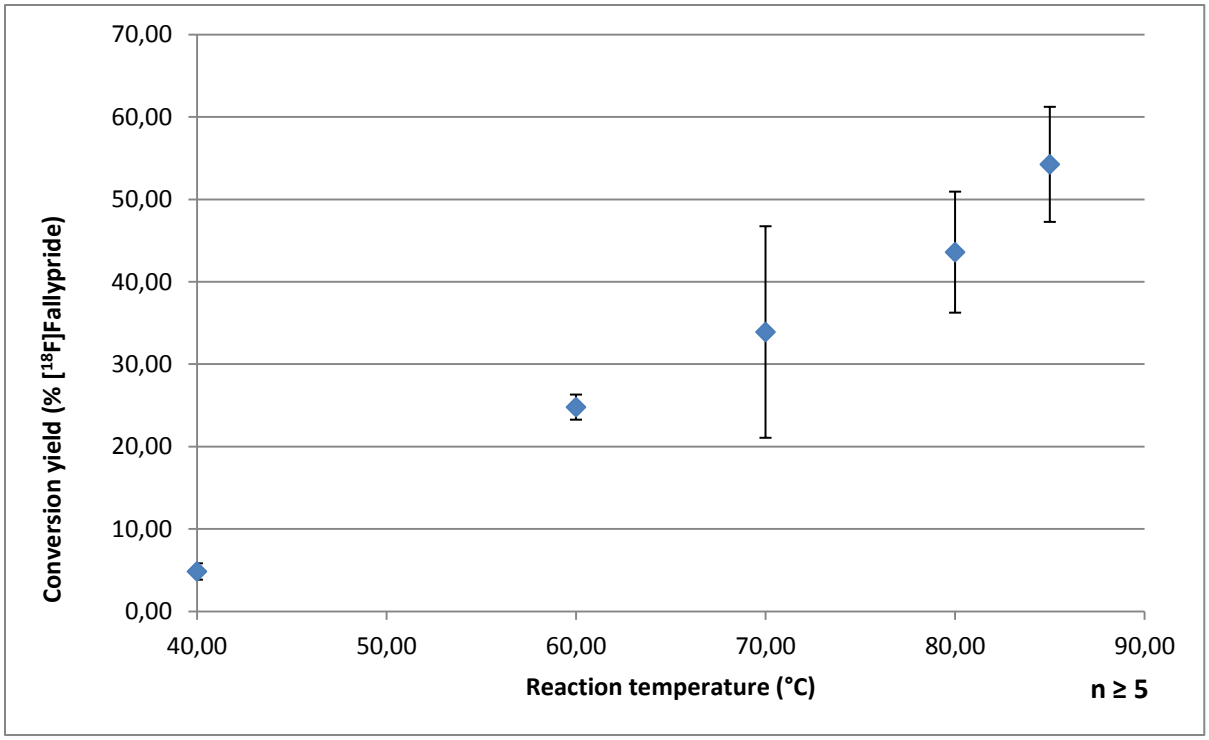

Fig. 3.1: Dependency of conversion yields of [^{18}F]Fallypride on reaction temperature at a constant precursor concentration of 5mg/mL, stirred for 15 minutes

Dependency of reaction yields on precursor concentration and reaction duration were tested at 70°C and varying reaction durations of 2, 5, 15 and 30 minutes. Three different precursor concentrations of 1mg/mL, 2.5mg/mL and 5mg/mL were used.

Mean conversion yields increased for all precursor concentrations with extension of the reaction time, reaching a maximum for precursor concentrations 1mg/mL and 5mg/mL at a reaction time of 15 minutes.

At a concentration of 2.5mg/mL, yields increased further when reaction duration was increased from 15 minutes to 30 minutes. (see Table 3.2 and Fig. 3.2)

Precursor concentration	Reaction duration (min.)	Total mean yield (%)	Standard deviation (%)
1mg/mL	2	2.4	1.9
	5	7.3	2.8
	15	16.5	3.4
	30	15.5	2.9
2.5mg/mL	2	5.3	2.9
	5	19.8	6.1
	15	27.5	3.5
	30	35.6	4.2
5mg/mL	2	6.6	3.0
	5	20.8	5.1
	15	36.1	12.5
	30	33.8	7.0

Table 3.2: Dependency of conversion yields upon reaction duration and precursor concentration at a constant reaction temperature of 70°C

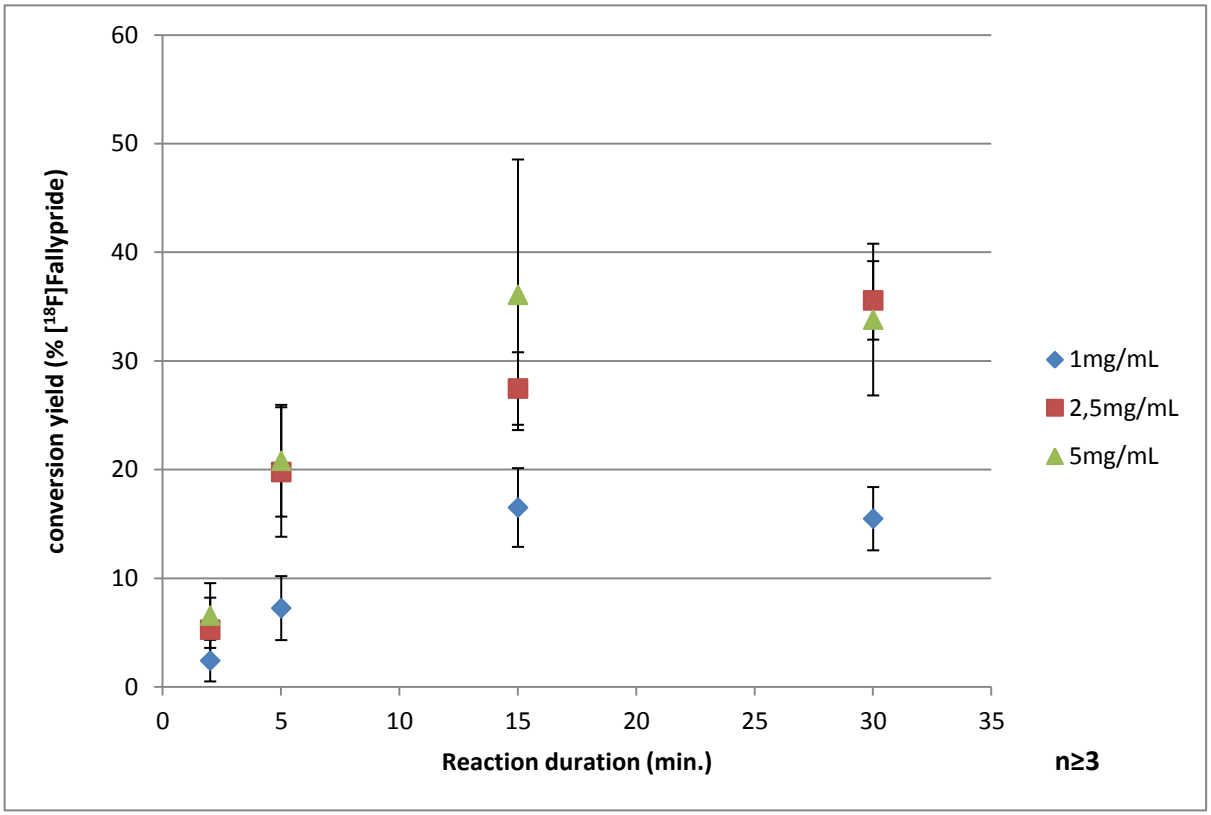

Fig. 3.2: Dependency of conversion yields upon reaction duration with various precursor concentrations (1; 2.5; 5 mg/mL) at a reaction temperature of 70°C

3.2 Microfluidic synthesis of [^{18}F]Fallypride

Microfluidic reactions showed no radiochemical incorporation at a reaction temperature of 26°C regardless of the used precursor concentration. At a temperature of 100°C, no conversion was observed with precursor concentrations lower than 1mg/mL. Only little conversion was detected at precursor concentrations of 2.5mg/mL and 5mg/mL in the reaction mixture. (5.3±0.3% respectively 1.02±0.3%)

At 140°C, conversion was achieved at all precursor concentrations and could be increased further by increasing the reaction temperature up to 180°C. (see Fig. 3.3). A distinct dependency upon the precursor concentration in the reaction mixture was also observed.

Maximum yields (91.6±1.0% incorporation of [^{18}F]fluoride) were observed at a precursor concentration of 2.5mg/mL, a reaction temperature of 180°C and an overall flow rate of 60µL/min (30µL/min per pump).

Precursor concentration	Reaction temperature (°C)	Total mean yield (%)	Standard deviation (%)
0.5mg/mL	26	0.0	0.0
	100	0.0	0.0
	140	17.5	2.3
	150	12.9	3.0
	160	16.2	0.9
	170	57.4	10.5
	180	56.5	1.4
1mg/mL	26	0.0	0.0
	100	0.0	0.0
	140	25.2	5.3
	150	35.9	12.6
	160	72.3	7.4
	170	72.9	9.8
	180	79.4	9.7
2.5mg/mL	26	0.0	0.0
	100	5.3	0.3
	140	47.3	1.0
	150	64.7	2.2
	160	79.7	1.6
	170	88.0	1.5
	180	91.6	1.0
5mg/mL	26	0.0	0.0
	100	1.0	0.3
	140	15.7	1.2
	150	38.3	8.9
	160	53.8	7.9
	170	81.5	1.0
	180	86.1	1.1

Table 3.3: Dependency of conversion upon reaction temperature and precursor concentration

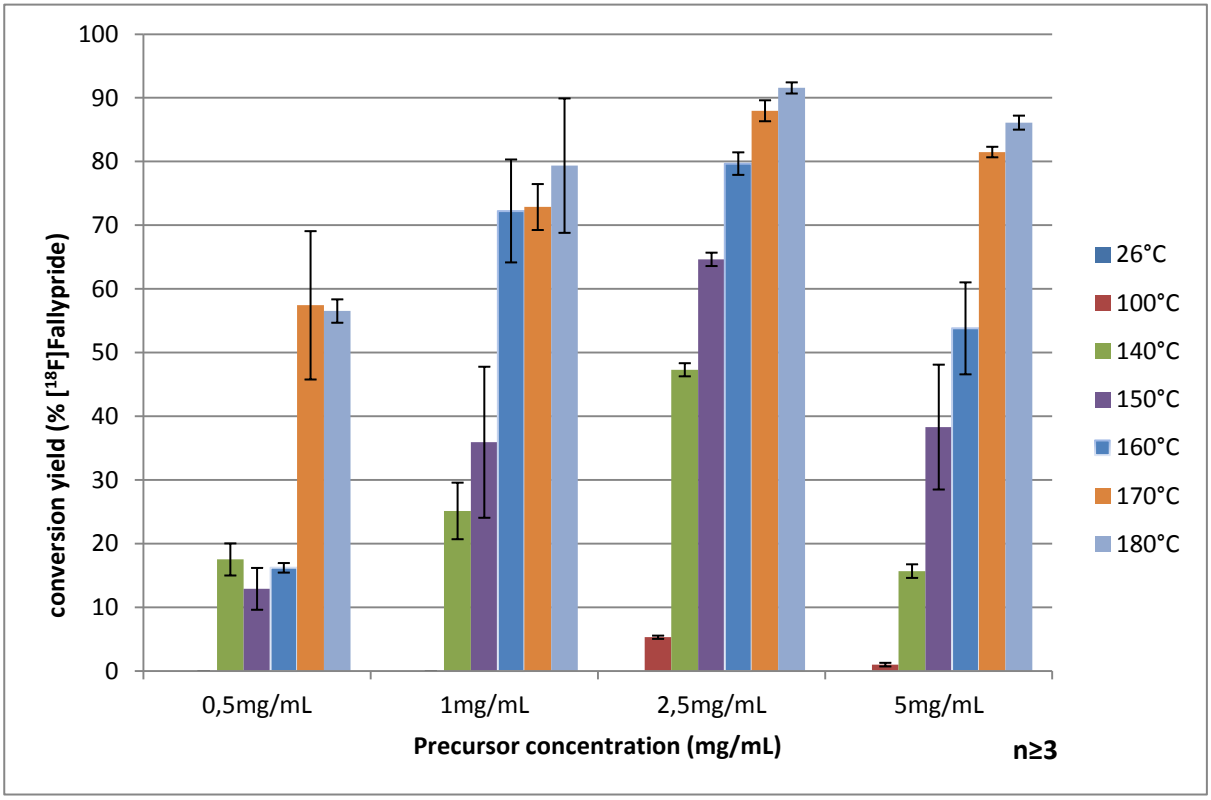

Fig. 3.3: Dependency of reaction yields upon precursor concentration and reaction temperature at an overall flow rate of 60µL/min

4 Discussion

Neither the evaluation of optimum reaction conditions regarding the synthesis of [^{18}F]Fallypride nor an analysis directly comparing vessel-based and microfluidic preparation of this substance have been presented in literature before.

Therefore, a direct comparison between these two approaches is presented here. Since the microfluidic synthesis of [^{18}F]Fallypride has been reviewed by Lu et al. in 2009 [78], the presented data will be compared with these results.

4.1 Vessel-based synthesis of [^{18}F]Fallypride

The influence of reaction temperature on yields was investigated at a temperature of 70°C and 15 minutes reaction duration. A distinct dependency of reaction yields upon reaction temperature was found. Yields fluctuated intensely at a reaction temperature of 70°C (standard deviation of ±12.5% from the mean yield, see Table 3.2).

Mukherjee et al. (1995) reported synthesis yields varying from 20-40% at a precursor concentration of 20mg/mL (3mg tosylate in 150µL acetonitrile) over a temperature range of 85-90°C and reaction duration of 30 minutes in acetonitrile. [69]

In a more recent work, Moon et al. (2010) were able to enhance radiochemical conversion by increasing the temperature and reducing the base component present in the reaction mixture. [79] They reported maximum conversion yields at 100°C and a reaction duration of 30 minutes (71±1.2%), but preferred the slightly lower yielding (68±1.6%) but faster reactions at 100°C and 10 minutes reaction duration.

In contrast to the work of Mukherjee et al., detailed reaction conditions were specified. However, none of the conventional procedures achieved more than 72.4% of radiochemical conversion.

In this work, maximum yields of 54.3±7.0% were found at a reaction temperature of 85°C, a precursor concentration of 5mg/mL and reaction duration of 15 minutes.

Due to the boiling point of acetonitrile (81.6°C at atmospheric pressure) reactions in acetonitrile can be problematic at this temperature, since solvent evaporation and radioactive contamination can occur if the reaction vessel is not tightly sealed.

The influence of precursor concentration and reaction duration on yields was tested at three different precursor concentrations of 1mg/mL, 2.5mg/mL and 5mg/mL at a reaction temperature of 70°C. This temperature was chosen deliberately due to the large yield fluctuations found during the temperature experiments (see chapter 3.1.1) to maximize the influence of factors other than reaction temperature on reaction yields.

At a precursor concentration of 1mg/mL RCIYs were low, not exceeding 16.5±3.4% at 15 minutes reaction duration. Reactions at a precursor concentration of 2.5mg/mL showed a distinct dependency upon reaction duration, with yields constantly increasing from a duration of 2 minutes up to 30 minutes, showing peak yields of 35.6±4.2% at reaction times of 30 minutes.

Summing up, ideal reaction conditions for the vessel-based synthesis of [^{18}F]Fallypride are a precursor concentration of 2.5mg/mL and a reaction duration of 30 minutes, yielding 35.6±4.2% of the product [^{18}F]Fallypride. Against expectations, an increase of precursor concentration from 2.5mg/mL to 5mg/mL did not result in substantial gain in reaction yields. Neither did an extension of reaction duration from 15 to 30 minutes for precursor concentrations of 1mg/mL and 5mg/mL.

4.2 Microfluidic synthesis of [^{18}F]Fallypride

The optimization of the microfluidic synthesis of [^{18}F]Fallypride has been described recently by Lu et al. (2009) [78]. In this article, two different precursor concentrations (2mg/mL and 4mg/mL) were tested, while in the presented study four different precursor concentrations were examined.

Reaction set-up was identical to the set-up used by Lu et al. In both set-ups, a microreactor of 2m length and 100µm diameter was used. The precursor to [^{18}F]fluoride ratio was 1:1 (v/v%) in all examinations. Precursor concentrations and bolus sizes used were different. Lu et al. used a precursor concentration of 2mg/mL respectively 10µL bolus size, while in the present study concentrations 0.5mg/mL, 1mg/mL, 2.5mg/mL and 5mg/mL with bolus sizes of 5-50µL were examined.

Since the difference between used precursor concentrations is minimal, results from 2.5mg/mL experiments from this study and 2mg/mL experiments presented in [78] will be compared.

The only difference between these set-ups was a back-pressure device, which was used in the presented work. This back-pressure device was placed behind the reactor to prevent solvent evaporation and boiling in the reactor at high temperatures.

Lu et al. reported decay-corrected radiochemical yields of 0-65% over a temperature range of 100-170°C. We found radiochemical yields of 0% below 100°C at all precursor concentrations. Stable and very high radiochemical yields were found at a reaction temperature of 180°C, while Lu et al. reported erratic yields for temperatures above 170°C. The deviation obviously resulted from the missing back-pressure device after the reactor.

Reaction temperature	2mg/mL (literature)	2.5mg/mL
< 100°C	0%	0%
100°C	0%	5.3±0.3%
140°C	~38%	47.3±1.0%
150°C	~40%	64.7±2.2%
160°C	~60%	79.7±1.6%
170°C	~65%	88.0±1.5%
180°C	erratic	91.6±1.0%

Table 4.1: Comparison of literature data using 2mg/mL precursor concentration and presented data using 2.5mg/mL precursor concentration.

The results indicate that only a precursor concentration of 2.5mg/mL produces stable and reproducible yields throughout the used temperature spectrum. Precursor concentrations below and also above 2.5mg/mL produced significant yield fluctuations at certain reaction temperatures.

4.2.1 Difficulties encountered using the Advion NanoTek LF system

Although the use of the Advion NanoTek LF system for radiosyntheses offers several advantages compared to conventional vessel-based synthesis, the system is still suffering from “teething troubles”.

A problem encountered often was the clogging of reactors. Particulate impurities from solvents led to the congestion of the system, causing an over-pressure failure. The system automatically stopped all actions to prevent pump damage. To restore the system it was often necessary to run several time consuming cleaning steps to remove potential particulate contaminations. In some cases, it was not possible to re-

open the reactor even after several cleaning runs. The reactor then had to be exchanged for a new one.

Another problem with reactors occurred with a batch of new reactors that started to leak after several syntheses. These reactors did not withstand the pressures occurring during syntheses, causing the connection between the reactor capillary and the pump lines to break. These reactors were exchanged free of charge by the manufacturer.

Additionally, the usability of the software interface (version 1.3.2) was not satisfactory, especially when programming routines in the proprierary programming language. This, however, has already been addressed in a recent software update. (version 1.4.0)

4.3 Comparison between vessel-based and microfluidic approach

Highest RCIYs of 54.3±7% were found at a precursor concentration of 5mg/mL at 85°C and reaction duration of 15 minutes in the vessel-based approach. Since reactions were held under pressure (up to 400psi/28bar), reaction temperatures could be increased up to 180°C in the Advion NanoTek LF without causing the solvent to boil. The increased reaction temperature made conversion yields of 91.6±1% at 2.5mg/mL precursor concentration in the reaction solution possible. The microfluidic approach overtops the results of the vessel-based synthesis approach by far. Also previously reported studies conducted with conventional set-ups, either automated [79] or manual [69], didn't reach such high conversion yields.

While the vessel-based approach necessitated reaction volumes of at least 250µL of precursor solution, the microfluidic approach used very small reaction volumes starting from 5µL up to maximally 50µL, leading to a reduction of precursor usage in the range of 20% up to 98% in comparison with the vessel-based approach.

In a typical optimization run using a precursor concentration of 2.5mg/mL, a minimum amount of 12.5µg (0.02µmol) up to a maximum amount of 125µg (0.2µmol) of precursor were applied. Reduction of precursor usage is an important advantage of this method, especially when rare or expensive precursor substances are used.

Another benefit of microfluidic systems is the feasibility of reaction optimizations at a fraction of the time needed with conventional methods. From a single batch of

precursor and radionuclide, multiple individual reactions (up to 40 in our set-up) can be carried out without any further time-consuming preparation or cleaning steps. The limit is only set by the volume of the used storage loops and the amount of radioactivity per batch needed for reliable detection in the used chromatographic assays. Using the built-in discovery mode of the Advion NanoTek LF system, reaction conditions can be quickly varied, enabling the evaluation of optimum reaction conditions for a reaction in a very short period of time.

When optimum reaction conditions have been established, reactions can be easily scaled up by using the batch mode to produce larger quantities of the desired radiotracer. Except from increasing the reaction volume, no changes in reaction parameters must be made for scaling up.

It is also possible to directly connect the product outlet of the Advion NanoTek LF system to an HPLC system or SPE cartridge for in-line product purification, yielding a ready-to-use product. Also, the use of an HPLC/MS-coupling for product purification and subsequent product identification has been reported.

5 Summary and outlook

During this diploma thesis, the synthesis and quality control of [^{18}F]Fallypride using two different approaches has been established. Although there were many problems concerning the handling of the microfluidic system, the system demonstrated its superiority in achievable radiochemical conversion yields. Obviously, this emerging technique is still suffering from “teething problems”. Apart from these problems, the system offers the opportunity of unprecedented radiochemical conversion yields and shorter reaction times. The syntheses conducted with the microfluidic system overtop the results of the vessel-based synthesis approach by far: in terms of yields, precursor usage and reaction duration.

For the vessel-based set-up, highest conversion yields of 54.3±7% were obtained at a precursor concentration of 5mg/mL and a reaction duration of 15 minutes at 85°C. At 70°C, reactions at a precursor concentration of 2.5mg/mL and a reaction duration of 30 minutes still yielded 35.6±4.2%, making this set-up the economically cheapest and thus most preferable.

With 2.5mg/mL of precursor used, the microfluidic technique yielded 91.6±1.0% of the product at 180°C using a 60µL/min overall flow rate. Since the vessel-based approach did not show as high radiochemical yields as the microfluidic approach, only the latter was automated, making direct interaction unnecessary. This is a big advantage in terms of radiation protection.

For the further use of [^{18}F]Fallypride in clinical or animal studies, the preparative HPLC purification and galenic formulation of the radiotracer (both published in [80]) need to be established at the production site using available standard procedures.

All in all, the successful implementation and optimization of the radiosynthesis of the important neuroimaging PET tracer, [^{18}F]Fallypride, was achieved.

6 Appendix: raw data

Raw data sets of the experimental series performed are presented in table 6.1.

Number of table	Description
	Vessel-based syntheses
6.2	Influence of reaction temperature on synthesis yields
6.3	Influence of precursor concentration and reaction duration on synthesis yields (1mg/mL tosyl-Fallypride)
6.4	Influence of precursor concentration and reaction duration on synthesis yields (2.5mg/mL tosyl-Fallypride)
6.5	Influence of precursor concentration and reaction duration on synthesis yields (5mg/mL tosyl-Fallypride)
	Microfluidic syntheses
6.6	Dependency of reaction yields on precursor concentration and reaction temperature (0,5mg/mL tosyl-Fallypride)
6.7	Dependency of reaction yields on precursor concentration and reaction temperature (1mg/mL tosyl-Fallypride)
6.8	Dependency of reaction yields on precursor concentration and reaction temperature (2.5mg/mL tosyl-Fallypride)
6.9	Dependency of reaction yields on precursor concentration and reaction temperature (5mg/mL tosyl-Fallypride)

Table 6.1: Overview of the raw data sets.

Temp. (°C)	Yield TLC 1 (%)	Yield TLC 2 (%)	Mean yield (%)	Total mean yield (%)	Standard deviation (%)
40	5.10	4.80	4.95	4.87	0.99
40	6.50	6.10	6.30		
40	3.70	3.40	3.55		
40	4.70	5.30	5.00		
40	4.50	4.60	4.55		
60	23.80	29.60	26.70	24.81	1.52
60	25.40	25.80	25.60		
60	22.40	24.20	23.30		
60	27.30	23.20	25.25		
60	23.60	22.80	23.20		
60	23.60	22.80	23.20		
70	26.10	23.80	24.95	36.09	12.45
70	24.50	22.30	23.40		
70	25.50	26.20	25.85		
70	47.80	52.20	50.00		
70	45.30	48.80	47.05		
70	51.80	55.00	53.40		
70	45.50	46.20	45.85		
70	44.30	47.40	45.85		
70	36.50	33.60	35.05		
70	23.40	24.10	23.75		
70	22.90	20.80	21.85		
85	44.20	45.70	44.95	54.26	6.98
85	56.60	54.60	55.60		
85	54.10	57.70	55.90		
85	44.20	47.90	46.05		
85	47.90	45.60	46.75		
85	64.70	57.00	60.85		
85	54.60	55.20	54.90		
85	56.30	60.60	58.45		
85	68.30	61.50	64.90		

Table 6.2: Vessel-based approach: influence of reaction temperature with 5mg/mL tosyl-Fallypride and 15 minutes reaction duration

Temp. (°C)	Reaction duration (min.)	Yield TLC 1 (%)	Yield TLC 2 (%)	Mean yield (%)	Total mean yield (%)	Standard deviation (%)
70	2	2.80	2.60	2.70	2.43	1.85
70	2	4.10	4.90	4.50		
70	2	4.10	5.30	4.70		
70	2	0.00	0.50	0.25		
70	2	1.70	2.10	1.90		
70	2	0.40	0.60	0.50		
70	5	11.00	11.90	11.45	7.26	2.83
70	5	9.50	10.30	9.90		
70	5	8.00	7.60	7.80		
70	5	4.50	4.30	4.40		
70	5	4.50	5.00	4.75		
70	5	5.70	4.80	5.25		
70	15	19.70	21.70	20.70	16.52	3.39
70	15	14.60	14.30	14.45		
70	15	15.60	13.20	14.40		
70	30	18.20	18.40	18.30	15.49	2.91
70	30	10.70	12.80	11.75		
70	30	15.70	18.70	17.20		
70	30	13.80	15.60	14.70		

Table 6.3: Vessel-based approach: influence of reaction duration with 1mg/mL tosyl-Fallypride stirred at 70°C

Temp. (°C)	Reaction duration (min.)	Yield TLC 1 (%)	Yield TLC 2 (%)	Mean yield (%)	Total mean yield (%)	Standard deviation (%)
70	2	2.5	3.6	3.05	5.27	2.93
70	2	2.3	2.7	2.5		
70	2	5.9	6.9	6.4		
70	2	8.5	11.1	9.8		
70	2	5.8	3.4	4.6		
70	5	23.9	32.4	28.15	19.78	6.07
70	5	24.4	28.2	26.3		
70	5	15.7	16.3	16		
70	5	17.1	15.2	16.15		
70	5	19.6	16.9	18.25		
70	5	14.5	13.2	13.85		
70	15	24.3	24.7	24.5	27.47	3.51
70	15	29.1	26.9	28		
70	15	22.6	24.7	23.65		
70	15	28.2	27	27.6		
70	15	31.7	34.5	33.1		
70	15	30.7	25.2	27.95		
70	30	26.2	35.4	30.8	35.58	4.20
70	30	35.7	33.9	34.8		
70	30	38.4	39.1	38.75		
70	30	37.2	38.7	37.95		

Table 6.4: Vessel-based approach: Influence of reaction duration with 2.5mg/mL tosyl-Fallypride stirred at 70°C

Temp. (°C)	Reaction duration (min.)	Yield TLC 1 (%)	Yield TLC 2 (%)	Mean yield (%)	Total mean yield (%)	Standard deviation (%)
70	2	11.40	10.40	10.90	6.58	2.98
70	2	8.30	8.60	8.45		
70	2	6.70	5.60	6.15		
70	2	3.90	3.60	3.75		
70	2	2.90	2.90	2.90		
70	2	7.40	7.20	7.30		
70	5	22.50	24.30	23.40	20.82	5.14
70	5	21.00	21.40	21.20		
70	5	14.20	13.40	13.80		
70	5	20.80	15.80	18.30		
70	5	28.10	26.70	27.40		
70	15	26.10	23.80	24.95	36.09	12.45
70	15	24.50	22.30	23.40		
70	15	25.50	26.20	25.85		
70	15	47.80	52.20	50.00		
70	15	45.30	48.80	47.05		
70	15	51.80	55.00	53.40		
70	15	45.50	46.20	45.85		
70	15	44.30	47.40	45.85		
70	15	36.50	33.60	35.05		
70	15	23.40	24.10	23.75		
70	15	22.90	20.80	21.85		
70	30	38.50	45.50	42.00	33.81	6.98
70	30	40.80	40.70	40.75		
70	30	28.20	29.60	28.90		
70	30	26.80	28.00	27.40		
70	30	28.60	31.40	30.00		

Table 6.5: Vessel-based approach: influence of reaction duration with 5mg/mL tosyl-Fallypride stirred at 70°C

Temp. (°C)	Precursor concentratipn	Yield TLC 1 (%)	Yield TLC 2 (%)	Mean yield (%)	Total mean yield (%)	Standard deviation (%)
26	0.5mg/mL	0.00	0.00	0.00	0.00	0.00
		0.00	0.00	0.00		
		0.00	0.00	0.00		
100	0.5mg/mL	0.00	0.00	0.00	0.00	0.00
		0.00	0.00	0.00		
		0.00	0.00	0.00		
140	0.5mg/mL	19.40	19.20	19.30	17.53	2.28
		15.20	14.10	14.65		
		18.60	18.70	18.65		
150	0.5mg/mL	16.00	17.40	16.70	12.92	2.98
		10.90	11.60	11.25		
		11.10	10.50	10.80		
160	0.5mg/mL	17.80	16.20	17.00	16.22	0.89
		15.80	15.20	15.50		
		16.50	15.80	16.15		
170	0.5mg/mL	71.60	68.40	70.00	57.43	10.48
		55.00	55.60	55.30		
		46.40	47.60	47.00		
180	0.5mg/mL	57.80	58.40	58.10	56.53	1.40
		56.20	54.80	55.50		
		56.70	55.30	56.00		

Table 6.6: Microfluidic approach: dependency of reaction yields upon reaction temperature at a constant precursor concentration of 0.5mg/mL tosyl-Fallypride in the reaction mixture and 60µL/min overall flow rate

Temp. (°C)	Precursor concentration	Yield TLC 1 (%)	Yield TLC 2 (%)	Mean yield (%)	Total mean yield (%)	Standard deviation (%)
26	1mg/mL	0.00	0.00	0.00	0.00	0.00
		0.00	0.00	0.00		
		0.00	0.00	0.00		
100	1mg/mL	0.00	0.00	0.00	0.00	0.00
		0.00	0.00	0.00		
		0.00	0.00	0.00		
140	1mg/mL	25.00	29.50	27.25	25.15	5.26
		25.00	31.30	28.15		
		16.20	23.90	20.05		
150	1mg/mL	21.50	25.20	23.35	35.93	12.57
		38.70	55.10	46.90		
		31.00	44.10	37.55		
160	1mg/mL	80.70	82.40	81.55	72.25	7.41
		66.90	67.00	66.95		
		65.80	70.70	68.25		
170	1mg/mL	63.80	76.90	70.35	72.87	9.79
		58.20	84.30	71.25		
		76.30	77.70	77.00		
180	1mg/mL	69.60	66.70	68.15	79.37	9.72
		85.90	92.30	89.10		
		79.70	82.00	80.85		

Table 6.7: Microfluidic approach: dependency of reaction yields upon reaction temperature at a constant precursor concentration of 1mg/mL tosyl-Fallypride in the reaction mixture and 60µL/min overall flow rate

Temp. (°C)	Precursor concentration	Yield TLC 1 (%)	Yield TLC 2 (%)	Mean yield (%)	Total mean yield (%)	Standard deviation (%)
26	2.5mg/mL	0.00	0.00	0.00	0.00	0.00
		0.00	0.00	0.00		
		0.00	0.00	0.00		
100	2.5mg/mL	5.40	5.80	5.60	5.32	0.33
		5.00	5.50	5.25		
		4.90	5.30	5.10		
140	2.5mg/mL	48.70	48.10	48.40	47.32	0.95
		46.20	46.50	46.35		
		47.10	47.30	47.20		
150	2.5mg/mL	66.70	61.10	63.90	64.65	2.19
		65.60	62.80	64.20		
		66.00	65.70	65.85		
160	2.5mg/mL	80.30	80.20	80.25	79.68	1.59
		77.50	77.90	77.70		
		81.10	81.10	81.10		
170	2.5mg/mL	89.90	89.80	89.85	87.98	1.51
		86.80	87.90	87.35		
		86.70	86.80	86.75		
180	2.5mg/mL	90.80	90.60	90.70	91.57	0.99
		91.10	92.00	91.55		
		93.30	91.60	92.45		

Table 6.8: Microfluidic approach: dependency of reaction yields upon reaction temperature at a constant precursor concentration of 2.5mg/mL tosyl-Fallypride in the reaction mixture and 60µL/min overall flow rate

Temp. (°C)	Precursor concentration	Yield TLC 1 (%)	Yield TLC 2 (%)	Mean yield (%)	Total mean yield (%)	Standard deviation (%)
26	5mg/mL	0.00	0.00	0.00	0.00	0.00
		0.00	0.00	0.00		
		0.00	0.00	0.00		
100	5mg/mL	0.50	0.90	0.70	1.02	0.30
		1.10	1.40	1.25		
		1.10	1.10	1.10		
140	5mg/mL	14.50	15.20	14.85	15.70	1.18
		16.90	16.90	16.90		
		14.30	16.40	15.35		
150	5mg/mL	26.50	27.50	27.00	38.32	8.91
		43.00	45.20	44.10		
		46.10	41.60	43.85		
160	5mg/mL	52.40	38.60	45.50	53.82	7.88
		59.20	55.70	57.45		
		58.00	59.00	58.50		
170	5mg/mL	81.50	79.60	80.55	81.50	0.98
		81.90	82.20	82.05		
		82.20	81.60	81.90		
180	5mg/mL	87.40	87.00	87.20	86.12	1.09
		85.30	84.70	85.00		
		86.80	85.50	86.15		

Table 6.9: Microfluidic approach: dependency of reaction yields upon reaction temperature at a constant precursor concentration of 5mg/mL tosyl-Fallypride in the reaction mixture and 60µL/min overall flow rate

7 Figures

8 Tables

9 References

[1]Soddy F. The Origins of the Conception of Isotopes. *Sci Mon* **1923**; 17: 305-317

[2]Lieser KH. Nuclear and Radiochemistry - Fundamentals and Applications. Wiley-VCH Verlag GmbH, Berlin Weinheim; Second Revised Edition: p6. (**2001**)

[3]Magill J PG, Galy J. Chart of the Nuclides. **2006**; Seventh Edition: p17.

[4]Lieser KH. Nuclear and Radiochemistry - Fundamentals and Applications. Wiley-VCH Verlag GmbH, Berlin Weinheim; Second Revised Edition: p20. (**2001**)

[5]Pfennig G K-NH, Seelmann-Eggebert W. Chart of the Nuclides, simplified and truncated. Sixth Edition: p1. (**1995**)

[6]Kassis AI Adelstein SJ. Radiobiologic principles in radionuclide therapy. *J Nucl Med* **2005**; 46 Suppl 1: 5S

[7]Chin PW Spyrou NM. Monte Carlo investigation of positron annihilation in medical positron emission tomography. *Nucl Instrum Meth A* **2007**; 580: 481-484

[8]Lieser KH. Nuclear and Radiochemistry - Fundamentals and Applications. Wiley-VCH Verlag GmbH, Berlin Weinheim; Second Revised Edition: p54. (**2001**)

[9]Lieser KH. Nuclear and Radiochemistry - Fundamentals and Applications. Wiley-VCH Verlag GmbH, Berlin Weinheim; Second Revised Edition: p112. (**2001**)

[10]Welch M, Redvanly CS. Handbook of Radiopharmaceuticals - Radiochemistry and Applications. John Wiley & Sons, Chichester; p93. (**2003**)

[11]Welch M, Redvanly CS. Handbook of Radiopharmaceuticals - Radiochemistry and Applications. **2003**; 89

[12]Welch M, Redvanly CS. Handbook of Radiopharmaceuticals - Radiochemistry and Applications. John Wiley & Sons, Chichester; p94. (**2003**)

[13]http://www.bnl.gov/bnlweb/history/tc-99m.asp. (October 22, 2010).

[14]Zolle I. Technetium-99m pharmaceuticals - Preparation and Quality Control in Nuclear Medicine. Springer, Berlin Heidelberg; p84. (**2007**)

[15]http://hyperphysics.phy-astr.gsu.edu/hbase/magnetic/cyclot.html. (October 12, 2010).

[16]Tipler P. Physics for Scientists and Engineers. Elsevier GmbH, Spektrum Akademischer Verlag, Munich; Third Edition, Extended Version: p825. (**2000**)

[17]Hess E, Blessing G, Coenen HH Qaim SM. Improved target system for production of high purity [18F]fluorine via the 18O(p,n)18F reaction. *Appl Radiat Isot* **2000**; 52: 1431-1440

[18]Wadsak W. Vorlesungsskript Medizinische Radiochemie 1. 375

[19]http://www.conradia.de/typo3temp/pics/0f321beed4.jpg. (March 31, 2011).

[20]Kowalsky RJ FS. Radiopharmaceuticals in Nuclear Pharmacy and Nuclear Medicine. American Pharmacists Association, Washington; Second Edition: p338. (**2004**)

[21]Turkington TG. Introduction to PET instrumentation. *J Nucl Med Technol* **2001**; 29: 4-11

[22]Welch M, Redvanly CS. Handbook of Radiopharmaceuticals - Radiochemistry and Applications. John Wiley & Sons, Chichester; p43. (**2003**)
[23]Lieser KH. Nuclear and Radiochemistry - Fundamentals and Applications. Wiley-VCH Verlag GmbH, Berlin Weinheim; Second Revised Edition: p378. (**2001**)
[24]Kilbourn M. Fluorine-18 labeling of radiopharmaceuticals. *Washington D.C.: National Academy Press* **1990**;
[25]Welch M, Redvanly CS. Handbook of Radiopharmaceuticals - Radiochemistry and Applications. John Wiley & Sons, Chichester; p44. (**2003**)
[26]Visser GWM, Bakker CNM, Herscheid JDM, Brinkman G Hoekstra A. The Chemical-Properties of [F-18] Acetylhypofluorite in Acetic-Acid Solution. *J Labelled Compd Rad* **1984**; 21: 1226-1226
[27]Chirakal R, Firnau G, Schrobilgen GJ, Mckay J Garnett ES. The Synthesis of [F-18] Xenon Difluoride from [F-18] Fluorine-Gas. *Int J Appl Radiat Is* **1984**; 35: 401-404
[28]Coenen HH. Fluorine-18 labeling methods: Features and possibilities of basic reactions. *Ernst Schering Res Found Workshop* **2007**; 20
[29]Coenen HH. Fluorine-18 labeling methods: Features and possibilities of basic reactions. *Ernst Schering Res Found Workshop* **2007**; 21
[30]Coenen HH. Fluorine-18 labeling methods: Features and possibilities of basic reactions. *Ernst Schering Res Found Workshop* **2007**; 22
[31]Hamacher K, Coenen HH Stocklin G. Efficient Stereospecific Synthesis of No-Carrier-Added 2-[F-18]-Fluoro-2-Deoxy-D-Glucose Using Aminopolyether Supported Nucleophilic-Substitution. *J Nucl Med* **1986**; 27: 235-238
[32]Coenen HH. Fluorine-18 labeling methods: Features and possibilities of basic reactions. *Ernst Schering Res Found Workshop* **2007**; 25
[33]DeWitt SH. Microreactors for chemical synthesis. *Curr Opin Chem Biol* **1999**; 3: 350-356
[34]Palmieri A, Ley SV, Hammond K, Polyzos A Baxendale IR. A microfluidic flow chemistry platform for organic synthesis: the Hofmann rearrangement. *Tetrahedron Lett* **2009**; 50: 3287-3289
[35]Carlsson A, Lindqvist M Magnusson T. 3,4-Dihydroxyphenylalanine and 5-hydroxytryptophan as reserpine antagonists. *Nature* **1957**; 180: 1200
[36]Aktories F, Hoffmann, Starke. Allgemeine und spezielle Pharmakologie und Toxikologie. Elsevier GmbH, Urban & Fischer Verlag, Munich; 10.Auflage: p188. (**2009**)
[37]Carlsson A. A paradigm shift in brain research. *Science* **2001**; 294: 1022
[38]Kebabian JW, Petzold GL Greengard P. Dopamine-sensitive adenylate cyclase in caudate nucleus of rat brain, and its similarity to the "dopamine receptor". *Proc Natl Acad Sci U S A* **1972**; 69: 2145-2149
[39]Kebabian JW Calne DB. Multiple Receptors for Dopamine. *Nature* **1979**; 277: 93-96

[40]Arias-Carrion O Poppel E. Dopamine, learning, and reward-seeking behavior. *Acta Neurobiol Exp (Wars)* **2007**; 67: 481-488

[41]Di Chiara G Bassareo V. Reward system and addiction: what dopamine does and doesn't do. *Curr Opin Pharmacol* **2007**; 7: 69-76

[42]Marsden CA. Dopamine: the rewarding years. *Br J Pharmacol* **2006**; 147 Suppl 1: S136-144

[43]Jaber M, Robinson SW, Missale C Caron MG. Dopamine receptors and brain function. *Neuropharmacology* **1996**; 35: 1503-1519

[44]Albanese A, Altavista MC Rossi P. Organization of central nervous system dopaminergic pathways. *J Neural Transm Suppl* **1986**; 22: 3

[45]Pierce RC Kumaresan V. The mesolimbic dopamine system: the final common pathway for the reinforcing effect of drugs of abuse? *Neurosci Biobehav Rev* **2006**; 30: 215-238

[46]Albanese A, Altavista MC Rossi P. Organization of central nervous system dopaminergic pathways. *J Neural Transm Suppl* **1986**; 22: 11

[47]Cools R. Dopaminergic modulation of cognitive function-implications for L-DOPA treatment in Parkinson's disease. *Neurosci Biobehav Rev* **2006**; 30: 1-23

[48]Van Rossum J. Significance of Dopamine-Receptor Blockade for Mechanism of Action of Neuroleptic Drugs. *Arch Int Pharmacod T* **1966**; 160: 492-&

[49]Seeman P, Chau-Wong M, Tedesco J Wong K. Brain receptors for antipsychotic drugs and dopamine: direct binding assays. *Proc Natl Acad Sci U S A* **1975**; 72: 4376-4380

[50]http://www.nibb.ac.jp/en/sections/imgs/sasaoka_fig.jpg. (April 4, 2011).

[51]Tatsch K. Imaging of the dopaminergic system in parkinsonism with SPET. *Nucl Med Commun* **2001**; 22: 819-827

[52]Bartenstein P. PET in neuroscience - Dopaminergic, GABA/benzodiazepine, and opiate system. *Nuklearmed-Nucl Med* **2004**; 43: 34

[53]Booij J Knol RJ. SPECT imaging of the dopaminergic system in (premotor) Parkinson's disease. *Parkinsonism Relat Disord* **2007**; 13 Suppl 3: S425-428

[54]Seibyl. Decreased single-photon emission computed tomographic {I-123}beta-CIT striatal uptake correlates with symptom severity in Parkinson's disease (vol 38, pg 589, 1995). *Ann Neurol* **1996**; 39: 417-417

[55]Bartenstein P. PET in neuroscience - Dopaminergic, GABA/benzodiazepine, and opiate system. *Nuklearmed-Nucl Med* **2004**; 43: 35

[56]Jackson DM Westlinddanielsson A. Dopamine-Receptors - Molecular-Biology, Biochemistry and Behavioral-Aspects. *Pharmacol Therapeut* **1994**; 64: 291-370

[57]Suhara T, Fukuda H, Inoue O, Itoh T, Suzuki K, Yamasaki T Tateno Y. Age-Related-Changes in Human D1-Dopamine Receptors Measured by Positron Emission Tomography. *Psychopharmacology* **1991**; 103: 41-45

[58]Farde L Hall H. Positron Emission Tomography - Examination of Chemical Transmission in the Living Human Brain - Development of Radioligands. *Arzneimittel-Forsch* **1992**; 42-1: 260-264

[59]Sedvall G, Karlsson P, Lundin A, Anvret M, Suhara T, Halldin C Farde L. Dopamine D-1 Receptor Number - a Sensitive Pet Marker for Early Brain Degeneration in Huntingtons-Disease. *Eur Arch Psy Clin N* **1994**; 243: 249-255

[60]Ginovart N, Lundin A, Farde L, Halldin C, Backman L, Swahn CG, Pauli S Sedvall G. PET study of the pre- and post-synaptic dopaminergic markers for the neurodegenerative process in Huntington's disease. *Brain* **1997**; 120: 503-514

[61]Rinne JO, Laihinen A, Nagren K, Bergman J, Solin O, Haaparanta M, Ruotsalainen U Rinne UK. Pet Demonstrates Different Behavior of Striatal Dopamine D-1 and D-2 Receptors in Early Parkinsons-Disease. *J Neurosci Res* **1990**; 27: 494-499

[62]Andersen PH, Gronvald FC, Hohlweg R, Hansen LB, Guddal E, Braestrup C Nielsen EB. Nnc-112, Nnc-687 and Nnc-756, New Selective and Highly Potent Dopamine D1 Receptor Antagonists. *European Journal of Pharmacology* **1992**; 219: 45-52

[63]Yang ZY, Perry B Mukherjee J. Fluorinated benzazepines .1. Synthesis, radiosynthesis and biological evaluation of a series of substituted benzazepines as potential radiotracers for positron emission tomographic studies of dopamine D-1 receptors. *Nuclear Medicine and Biology* **1996**; 23: 793-805

[64]Kaiser C Jain T. Dopamine-Receptors - Functions, Subtypes and Emerging Concepts. *Med Res Rev* **1985**; 5: 145-229

[65]Volkow ND, Fowler JS, Gatley SJ, Logan J, Wang GJ, Ding YS Dewey S. PET evaluation of the dopamine system of the human brain. *J Nucl Med* **1996**; 37: 1242-1256

[66]Christian BT, Narayanan TK, Shi BZ Mukherjee J. Quantitation of striatal and extrastriatal D-2 dopamine receptors using PET imaging of [F-18]fallypride in nonhuman primates. *Synapse* **2000**; 38: 71-79

[67]Slifstein M, Hwang DR, Huang YY, Guo NN, Sudo Y, Narendran R, Talbot P Laruelle M. In vivo affinity of [F-18]fallypride for striatal and extrastriatal dopamine D-2 receptors in nonhuman primates. *Psychopharmacology* **2004**; 175: 274-286

[68]Mukherjee J. Fluorinated Benzamide Neuroleptics .2. Synthesis and Radiosynthesis of (S)-N-[(1-Ethyl-2-Pyrrolidinyl)Methyl]-5-(3-[F-18]Fluoropropyl)-3-Substituted-2-Methoxybenzamides. *Appl Radiat Isotopes* **1991**; 42: 713-721

[69]Mukherjee J, Yang ZY, Das MK Brown T. Fluorinated benzamide neuroleptics--III. Development of (S)-N-[(1-allyl-2-pyrrolidinyl)methyl]-5-(3-[18F]fluoropropyl)-2, 3-dimethoxybenzamide as an improved dopamine D-2 receptor tracer. *Nucl Med Biol* **1995**; 22: 283-296

[70]Mathis CA, Bishop JE, Gerdes JM, Whitney JM, Brennan KM Jagust WJ. Synthesis and Evaluation of High-Affinity, Aryl-Substituted [F18]Fluoropropylbenzamides for Dopamine D-2-Receptor Studies. *Nuclear Medicine and Biology* **1992**; 19: 571-&

[71]Leung K. (S)-N-((1-Allyl-2-pyrrolidinyl)methyl)-5-(3-[18F]fluoropropyl)-2,3-dimethoxybenzamide

[[^{18}F]Fallypride]. *Molecular Imaging and Contrast Agent Database (MICAD) [database online]. Bethesda (MD): National Library of Medicine (US), NCBI; 2004-2010. Available from: http://micad.nih.gov.* **2008**;

[72]Riccardi P, Li R, Ansari MS, Zald D, Park S, Dawant B, Anderson S, Doop M, Woodward N, Schoenberg E, Schmidt D, Baldwin R Kessler R. Amphetamine-induced displacement of [F-18] fallypride in striatum and extrastriatal regions in humans. *Neuropsychopharmacol* **2006**; 31: 1016-1026

[73]Grunder G, Landvogt C, Vernaleken I, Buchholz HG, Ondracek J, Siessmeier T, Hartter S, Schreckenberger M, Stoeter P, Hiemke C, Rosch F, Wong DF Bartenstein P. The striatal and extrastriatal D2/D3 receptor-binding profile of clozapine in patients with schizophrenia. *Neuropsychopharmacol* **2006**; 31: 1027-1035

[74]Cai LS, Lu SY Pike VW. Chemistry with [F-18]fluoride ion. *Eur J Org Chem* **2008**; 2853-2873

[75]Kemp DD Gordon MS. Theoretical study of the solvation of fluorine and chlorine anions by water. *J Phys Chem A* **2005**; 109: 7688-7699

[76]Renard JA Oberg AG. Ternary Systems - Water-Acetonitrile-Salts. *J Chem Eng Data* **1965**; 10: 152-&

[77]Ungersboeck J, Philippe C, Mien LK, Haeusler D, Shanab K, Lanzenberger R, Spreitzer H, Keppler BK, Dudczak R, Kletter K, Mitterhauser M Wadsak W. Microfluidic preparation of [18F]FE@SUPPY and [18F]FE@SUPPY:2--comparison with conventional radiosyntheses. *Nucl Med Biol* **2011**; 38: 427-434

[78]Lu S, Giamis AM Pike VW. Synthesis of [F]fallypride in a micro-reactor: rapid optimization and multiple-production in small doses for micro-PET studies. *Curr Radiopharm* **2009**; 2: nihpa81093

[79]Moon BS, Park JH, Lee HJ, Kim JS, Kil HS, Lee BS, Chi DY, Lee BC, Kim YK Kim SE. Highly efficient production of [(18)F]fallypride using small amounts of base concentration. *Appl Radiat Isot* **2010**; 68: 2279-2284

[80]Mukherjee J, Yang ZY, Brown T, Lew R, Wernick M, Ouyang XH, Yasillo N, Chen CT, Mintzer R Cooper M. Preliminary assessment of extrastriatal dopamine D-2 receptor binding in the rodent and nonhuman primate brains using the high affinity radioligand, F-18-fallypride. *Nuclear Medicine and Biology* **1999**; 26: 519-527

M i c h a e l Z e i e r

C u r r i c u l u m v i t a e

Personal data

Name:	Michael Zeier
Date of birth:	18.12.1982
Address:	Kirchengasse 48/2, 1070 Wien
Nationality:	Austria
eMail:	michael.zeier@reflex.at

Education

1989-1993	Primary School in Traun, Upper Austria
1993-2001	High School (Bundesrealgymnasium Traun),
2001	Graduation with distinction
2001-2002	Military service in Hörsching, Upper Austria
2002-2003	Studies of technical physics at the University of Linz
2003-2011	Studies of Pharmacy at the University of Vienna

Foreign languages

German: native language

English: fluent in spoken and written

Italian: basic communication skills

Scientific work

Collaborative work at the poster **Comparison of "conventional" radiosynthesis and microfluidic preparation of [^{18}F]FE@SUPPY:** Ungersboeck, J.; Mien, L.; Mitterhauser, M.; Holley, A.; **Zeier, M**.; Dudczak, R.; Kletter, K.; Keppler, B.; Wadsak, W.; Poster presentation at EANM, October 2010.

Practical experience

July 2006	Internship at the „Ikarus Apotheke" in Hörsching, Upper Austria
2007-2011	Elected member of the Pharmacy Students Union of the University of Vienna